Surveillance Face Recognition Challenge

Zhiyi Cheng · Xiatian Zhu · Shaogang Gong

Abstract Face recognition (FR) is one of the most extensively investigated problems in computer vision. Recently we have witnessed significant progress in FR with the help of deep learning algorithms and larger scale datasets particularly those *constrained* social media web images, e.g. high-resolution photos of celebrity faces taken by professional photo-journalists. However, the more challenging FR in *unconstrained* and *low-resolution* surveillance images remains open and under-studied.

To stimulate the development of innovative FR methods effective and robust for low-resolution surveillance facial images, we introduce a new Surveillance Face Recognition Challenge, namely *QMUL-SurvFace*. This benchmark is the *largest* to date and more importantly the only *true* surveillance FR benchmark to our best knowledge. The low-resolution facial images are not synthesised by artificial down-sampling of high-resolution imagery but drawn from real surveillance videos. This benchmark has 463,507 facial images of 15,573 unique identities captured in uncooperative surveillance scenes over wide space and time. Consequently, QMUL-SurvFace presents a true-performance surveillance FR challenge characterised by low-resolution, motion blur, uncontrolled poses, varying occlusion, poor illumination, and background clutters.

On the QMUL-SurvFace challenge, we benchmark the FR performances of five representative deep learning face recognition models (DeepID2, CentreFace, VggFace, FaceNet, and SphereFace), in comparison to existing benchmarks. We show that the current state of the arts are still *far from being satisfactory* to tackle the under-investigated surveillance FR problem. In particular, we demonstrate a surprisingly large gap in FR performance between existing celebrity photoshot benchmarks (e.g. MegaFace) and QMUL-SurvFace. For example, the CentreFace model only yields 29.9% in Rank-1 rate on QMUL-SurvFace, *vs* a much higher performance at 65.2% on MegaFace in a closed-set test. Besides, open-set FR is shown more challenging but required for surveillance scenarios due to the presence of a large number of non-target people (distractors) in public space. This is indicated by weak FR performances on QMUL-SurvFace, e.g. the top-performer CentreFace achieves 13.8% *success rate* (at Rank-20) at the 10% *false alarm rate*.

Moreover, we extensively investigate the challenging low-resolution problem inherent to the surveillance facial imagery by testing different combining methods of image super-resolution and face recognition models on both web and surveillance datasets. Our evaluations suggest that current super-resolution methods are ineffective in improving low-resolution FR performance, although they have been shown useful to synthesise high frequency details for low-resolution web images.

Finally, we discuss a number of open research directions and problems that need to be addressed for solving the surveillance FR challenge. The QMUL-SurvFace challenge is publicly available at https://qmul-survface.github.io/.

Zhiyi Cheng and Shaogang Gong
School of Electrical Engineering and Computer Science, Queen Mary University of London, London E1 4NS, UK.
E-mail: {z.cheng, s.gong}@qmul.ac.uk

Xiatian Zhu
Vision Semantics Limited, London E1 4NS, UK.
E-mail: eddy@visionsemantics.com

Fig. 1: Example comparisons of (**Left**) *web face images* from five standard face recognition challenges and (**Right**) *native surveillance face images* from typical public surveillance scenes in real-world applications.

1 Introduction

Face recognition (FR) is a well established research problem in computer vision with the objective to recognise human identities (IDs) by their facial images (Zhao et al, 2003). There are other visual recognition based biometrics approaches to human identification, for example, whole-body person re-identification (Gong et al, 2014), iris recognition (Phillips et al, 2010), gait recognition (Sarkar et al, 2005), and fingerprint recognition (Maltoni et al, 2009). Among these, FR is considered as one of the more convenient and non-intrusive means for a wide range of identification applications from law enforcement and information security to business, entertainment and e-commerce (Wechsler et al, 2012). This is due to one fact that face appearance is more reliable and stable than clothing appearance, provided that facial images are visible.

The FR problem has been extensively studied over the past few decades since 1970s, and increasingly deployed in social applications within the last five years. In 2016 alone, there were over 77,300 FR publications including patents by Google Scholar. In particular, the last few years have witnessed FR performance on high-resolution good quality web images reaching a level arguably better than the humans, e.g. 99.83% for 1:1 face verification on the LFW challenge and 99.801% for 1:N face identification on the million-scale MegaFace challenge. Commercial FR products have become more mature and appeared increasingly in our daily life, e.g. web photo-album, online e-payment, and smart-phone e-banking, with such a trend accelerating at larger scales. One driving force behind the FR success is the synergistic and rapid advances in neural network based deep learning techniques, large facial imagery benchmarks, and powerful computing devices. The progress is advancing rapidly under the joint efforts of both the academic and industrial communities. One may argue then: "*The state-of-the-art FR algorithms, especially with the help of deep learning on large scale data, have reached a sufficient level of maturity and application readiness, evidenced by almost saturated performances on large scale public benchmark challenges*[1]. *Therefore, the FR problem should be considered as "solved" and the remaining efforts lie mainly in system production engineering.*"

However, as shown in this study, current FR methods scale poorly to natively noisy and low-resolution images (not synthesised by down-sampling), that are typified by facial data captured in *unconstrained wide-field surveillance videos and images*, perhaps one of the most important FR application fields in practice. Specifically, we demonstrate that FR in the typical surveillance images is far away from being satisfactory especially at a large scale. Unlike recognising high-resolution web photoshot images with limited noise, the problem of surveillance FR remains extremely challenging and open. This is a surprise because surveillance video data are characterised by low-resolution imagery with heavy noise, subject to poor imaging conditions giving rise to unconstrained pose, expression, occlusion, lighting and background clutter (Fig. 1).

In the literature, the *surveillance face recognition* problem is significantly under-studied in comparison to FR on web photoshots. Whilst *web face recognition* is popular and commercially attractive due to the proliferation of social media and e-commerce on smart-phones and various digital devices, solving the surveillance FR challenge is critical for public safety and law enforcement applications. A major reason for lacking the development of robust and scalable FR models suitable for surveillance scenes is the lack of large scale true surveillance facial imagery benchmark, in contrast to the rich availability of high-resolution web photoshot FR benchmarks (Table 1). For example, there are 4,753,320 web face images from 672,057 face IDs in the MegaFace2

---

[1] The FR performance differences among top-performing models are very marginal and negligible (see Table 2).

benchmark[2] (Nech and K-S, 2017). This is made possible by easier collection and labelling of large scale facial images in the public domain from the Internet.

On the contrary, it is prohibitively expensive and less feasible to construct large scale *native* surveillance facial imagery data as a benchmark for wider studies, due both to largely restricted data access and very tedious data labelling at high costs. Currently, the largest surveillance FR challenge benchmark is the UnConstrained College Students (UCCS) dataset[3] (Günther et al, 2017), which contains 100,000 face images from 1,732 face IDs, at a significantly smaller scale than the MegaFace celebrities photoshot dataset. However, the UCCS is limited and only semi-native due to being captured by a high-resolution camera at a single location. In this study, we show that: (1) The state-of-the-art deep learning based FR models trained on large scale high-quality benchmark datasets such as the MegaFace generalise poorly to native low-quality surveillance face recognition tasks; (2) The FR performance test on artificially synthesised low-resolution images does not well reflect the true challenges of native surveillance FR in system deployments; (3) The image super-resolution models suffer the lack of high-resolution surveillance facial images which are necessary for model training, apart from the domain distribution shift between web and surveillance data.

In this study, we provide a more realistic and large scale *Surveillance Face Recognition Challenge* than what is currently available in the public domains. That is, recognising a person's identity by natively low-resolution surveillance facial images taken from unconstrained public scenes. We make three contributions as follows:
(I) We construct a dataset of large scale face IDs with *native* surveillance facial imagery data for model development and evaluation. Specifically, we introduce the *QMUL-SurvFace* challenge, containing 463,507 face images of 15,573 IDs. To our best knowledge, this is the largest sized dataset for surveillance FR challenge, with *native* low-resolution surveillance facial images captured by unconstrained wide-field cameras at distances. This benchmark dataset is constructed by data-mining 17 public domain person re-identification datasets (Table 4) using a deep learning face detection model, so to assemble a large pool of labelled surveillance face images in a *cross-problem* data re-purposing principle. A unique feature of this new surveillance FR benchmark is the provision of cross-location (cross camera views) ID label annotations, available from the source person re-identification datasets. This cross-view labelling information is useful for open-set FR test.

(II) We benchmark five representative deep learning FR models (Liu et al, 2017, Parkhi et al, 2015, Schroff et al, 2015, Sun et al, 2014a, Wen et al, 2016) for both face identification and verification. In contrast to existing FR challenges typically considering a *closed-set* setting, we particularly evaluate these algorithms in performing a more realistic *open-set* surveillance FR task, originally missing in the previous studies. The closed-set test assumes the existence of every probe face ID in the gallery set so a true-match always exists for each probe, whilst the open-set test does not, respecting realistic large surveillance FR scenarios.
(III) We investigate the effectiveness of existing FR models on native low-resolution surveillance imagery data by exploiting simultaneously image super-resolution (Dong et al, 2014, 2016, Kim et al, 2016a, Lai et al, 2017, Tai et al, 2017) and FR models. We study different combinations of super-resolution and FR models including independent and joint training schemes. We further compare model performances on MegaFace and UCCS benchmarks to give better understanding of the unique characteristics of QMUL-SurvFace. We finally provide extensive discussions on future research directions towards solving the surveillance FR challenge.

2 Related Work

In this section, we review and discuss the representative FR challenges (Sec. 2.1) and methods (Sec. 2.2) in the literature. In Sec. 2.2, we focus on the models closely related to the surveillance FR challenge including recent deep learning algorithms. More general and extensive reviews can be found in other surveys (Abate et al, 2007, Adini et al, 1997, Chang et al, 2005, Chellappa et al, 1995, Daugman, 1997, Ersotelos and Dong, 2008, Kong et al, 2005, Prado et al, 2016, Samal and Iyengar, 1992, Tan et al, 2006, Wang et al, 2014b, Zhao et al, 2003, Zou et al, 2007) and books (Gong et al, 2000, Li and Jain, 2011, Wechsler, 2009, Wechsler et al, 1998, 2012, Zhao and Chellappa, 2011, Zhou et al, 2006).

2.1 Face Recognition Challenges

An overview of representative FR challenges and benchmarks are summarised in Table 1. Specifically, early challenges focus on *small-scale constrained* FR scenarios with limited number of images and IDs (Belhumeur et al, 1997, Georghiades et al, 2001, Gross et al, 2010, Messer et al, 1999, Phillips et al, 2010, Samaria and Harter, 1994, Sim et al, 2002). They provide neither sufficient appearance variation and diversity for robust model training, nor practically solid test benchmarks.

Table 1: The statistics of representative publicly available face recognition benchmarks. Celeb: Celebrity.

Challenge	Year	IDs	Images	Videos	Subject	Surveillance?
Yale (Belhumeur et al, 1997)	1997	15	165	0	Cooperative	No
QMUL-MultiView (Gong et al, 2000)	1998	25	4,450	5	Cooperative	No
XM2VTS (Messer et al, 1999)	1999	295	0	1,180	Cooperative	No
Yale B (Georghiades et al, 2001)	2001	10	5,760	0	Cooperative	No
CMU PIE (Sim et al, 2002)	2002	68	41,368	0	Cooperative	No
Multi-PIE (Gross et al, 2010)	2010	337	750,000	0	Cooperative	No
Morph (Ricanek and Tesafaye, 2006)	2006	13,618	55,134	0	Celeb (Web)	No
LFW (Huang et al, 2007)	2007	5,749	13,233	0	Celeb (Web)	No
YouTube Wolf et al (2011)	2011	1,595	0	3,425	Celeb (Web)	No
WDRef (Chen et al, 2012)	2012	2,995	99,773	0	Celeb (Web)	No
FaceScrub (Ng and Winkler, 2014)	2014	530	100,000	0	Celeb (Web)	No
CASIA (Yi et al, 2014)	2014	10,575	494,414	0	Celeb (Web)	No
CelebFaces (Sun et al, 2014b)	2014	10,177	202,599	0	Celeb (Web)	No
IJB-A (Klare et al, 2015)	2015	500	5,712	2,085	Celeb (Web)	No
VGGFace (Parkhi et al, 2015)	2015	2,622	2.6M	0	Celeb (Web)	No
UMDFaces (Bansal et al, 2016)	2016	8,277	367,888	0	Celeb (Web)	No
CFP (Sengupta et al, 2016)	2016	500	7,000	0	Celeb (Web)	No
UMDFaces (Bansal et al, 2016)	2016	8,277	367,888	0	Celeb (Web)	No
MS-Celeb-1M (Guo et al, 2016a)	2016	99,892	8,456,240	0	Celeb (Web)	No
UMDFaces-Videos (Bansal et al, 2017)	2017	3,107	0	22,075	Celeb (Web)	No
IJB-B (Whitelam et al, 2017)	2017	1,845	11,754	7,011	Celeb (Web)	No
VGGFace2 (Cao et al, 2017b)	2017	9,131	3.31M	0	Celeb (Web)	No
MegaFace2 (Nech and K-S, 2017)	2017	672,057	4,753,320	0	Non-Celeb (Web)	No
FERET (Phillips et al, 2000)	1996	1,199	14,126	0	Cooperative	No
FRGC (Phillips et al, 2005)	2004	466+	50,000+	0	Cooperative	No
CAS-PEAL (Gao et al, 2008)	2008	1,040	99,594	0	Cooperative	No
PaSC (Beveridge et al, 2013)	2013	293	9,376	2,802	Cooperative	No
FRVT(Visa) (Grother et al, 2017)	2017	$O(10^5)$	$O(10^5)$	0	Cooperative	No
FRVT(Mugshot) (Grother et al, 2017)	2017	$O(10^5)$	$O(10^6)$	0	Cooperative	No
FRVT(Selfie) (Grother et al, 2017)	2017	<500	<500	0	Cooperative	No
FRVT(Webcam) (Grother et al, 2017)	2017	<1,500	<1,500	0	Cooperative	No
FRVT(Wild) (Grother et al, 2017)	2017	$O(10^3)$	$O(10^5)$	0	Uncooperative	No
FRVT(Child Exp) (Grother et al, 2017)	2017	$O(10^3)$	$O(10^4)$	0	Uncooperative	No
SCface (Grgic et al, 2011)	2011	130	4,160	0	Cooperative	Yes
COX (Huang et al, 2015)	2015	1,000	1,000	3,000	Cooperative	Yes
UCCS (Günther et al, 2017)	2017	1,732	14,016+	0	Uncooperative	Yes
QMUL-SurvFace	2018	15,573	463,507	0	Uncooperative	Yes

In 2007, the seminal Labeled Faces in the Wild (LFW) challenge (Huang et al, 2007) was proposed and started to shift the community towards recognising unconstrained celebrity faces by providing web face images and a standard performance evaluation protocol. LFW has contributed significantly to a spurring of interest and progress in FR. This trend towards large datasets has been amplified by the creation of even larger FR benchmarks such as CASIA (Yi et al, 2014), CelebFaces (Sun et al, 2014b), VGGFace (Parkhi et al, 2015), MS-Celeb-1M (Guo et al, 2016a), MegaFace (K-S et al, 2016) and MegaFace2 (Nech and K-S, 2017). Thus far, it seems that the availability of large training and test data benchmark for web photoshot images has been addressed.

With such large benchmark challenges, FR accuracy in good quality images has reached an unprecedented level by deep learning. For example, the FR performance has reached 99.83% (face verification) on LFW and 99.801% (face identification) on MegaFace. However, this dose not scale to *native* low-resolution surveillance facial imagery data captured in unconstrained camera views (see Sec. 5.1). This is due to two reasons: (1) Existing FR challenges such as LFW have varying degrees of data selection bias (near-frontal pose, less motion blur, good illumination); and (2) Deep learning methods are often domain-specific (i.e. only generalise well to face images similar to the training data) On the other hand, there is big difference in facial images between a web photoshot view and a surveillance view in-the-wild (Fig. 1).

Research on surveillance FR has made little progress since the early days in 1996 when the well-known FERET challenge was launched (Phillips et al, 2000). It is understudied by large, with a very few benchmarks available. One of the major obstacles is the difficulty of establishing a large scale surveillance FR challenge due to the high cost and limited feasibility in collecting surveillance facial imagery data and exhaustive facial ID an-

notation. Even in the FERET dataset, only simulated (framed) surveillance face images were collected in most cases with carefully controlled imaging settings, therefore it provides a much better facial image quality than those from native surveillance videos.

A notable recent study introduced the UCCS face challenge (Günther et al, 2017), which is currently the largest surveillance FR benchmark in the public domain. The UCCS facial images were captured from a long-range distance without subjects' cooperation (unconstrained). The faces in these images are of various poses, blurriness and occlusion (Fig. 9(b)). This benchmark represents a relatively realistic surveillance FR scenario in comparison to FERET. However, the UCCS images were captured at high-resolution from a single camera view[4], therefore providing significantly more facial details with less viewing angle variations. Moreover, UCCS is small in size, particularly in term of the face ID numbers (1,732), statistically limited for evaluating surveillance FR challenge (Sec. 5.1). In this study, we address the limitations of UCCS by constructing a larger scale natively low-resolution surveillance FR challenge, the QMUL-SurvFace benchmark. It consists of 463,507 real-world surveillance face images of 15,573 different IDs captured from a diverse source of public spaces (Sec. 3).

2.2 Face Recognition Methods

We provide a brief review on the vast number of existing FR algorithms, including hand-crafted, deep learning, and low-resolution methods. The low-resolution FR methods are included for discussing the state-of-the-art in handling poor image quality. We also discuss image super-resolution (hallucination) techniques for enhancing image fidelity and improving FR performance on low-resolution imagery data.

(I) Hand Crafted Methods. Most early FR methods rely on hand-crafted features (e.g. Color Histogram, LBP, SIFT, Gabor) and matching model learning algorithms (e.g. discriminative margin mining, subspace learning, dictionary based sparse coding, Bayesian modelling) (Ahonen et al, 2006, Belhumeur et al, 1997, Cao et al, 2013, Chen et al, 2012, 2013, Liu and Wechsler, 2002, Tan and Triggs, 2010, Turk and Pentland, 1991, Wolf and Levy, 2013, Wright et al, 2009, Zhang et al, 2007). These methods are often inefficient subject to heavy computational cost of high-dimensional feature representations and complex image preprocessing. Moreover, they also suffer from sub-optimal recognition

generalisation particularly in a large sized data when there are significant facial appearance variations. This is jointly due to weak representation power (human domain knowledge used in hand-crafting features is limited and incomplete) and the lack of end-to-end interaction learning between feature extraction and model inference.

(II) Deep Learning Methods. In the past five years, FR models based on deep learning, particularly convolutional neural networks (CNNs) (K-S et al, 2016, Klare et al, 2015, Liu et al, 2017, Masi et al, 2016, Parkhi et al, 2015, Schroff et al, 2015, Sun et al, 2014c, Taigman et al, 2014, Wen et al, 2016), have achieved remarkable success (Table 2). This paradigm benefits from superior network architectures (He et al, 2016, Krizhevsky et al, 2012, Simonyan and Zisserman, 2015, Szegedy et al, 2015) and optimisation algorithms (Schroff et al, 2015, Sun et al, 2014c, Wen et al, 2016). Deep FR methods naturally address the limitations of hand-crafted alternatives by jointly learning face representation and matching model end-to-end. To achieve good performance, a large set of labelled face images is usually necessary to train the millions of parameters of deep models. This can be commonly satisfied by using millions of web face images collected and labelled (filtered) from the Internet sources. Consequently, modern FR models are often trained, evaluated and deployed on web face datasets (Table 1 and Table 2).

While the web FR performance achieves an unprecedented level, it remains unclear how well the state-of-the-art methods generalise to poor quality surveillance facial data. Intuitively, more challenges are involved in the surveillance FR scenario due to three reasons: **(1)** Surveillance face images contain much less appearance details with poorer quality and lower resolution (Fig. 1), thus hindering the FR performance. **(2)** Deep models are highly domain-specific and likely yield big performance degradation in cross-domain deployments. This is particularly so when the domain gap between the training and test data is large, such as web and surveillance faces. In such cases, transfer learning is challenging (Pan and Yang, 2010). The challenge can be further increased by the scarcity of labelled surveillance data. **(3)** Instead of the closed-set search considered in most existing methods, FR in surveillance scenarios is intrinsically open-set where the probe face ID is not necessarily present in the gallery. This brings about a significant challenge by additionally requiring the FR system to accurately reject non-target people (i.e. distractors) whilst simultaneously not missing target IDs. Therefore, open-set FR is more challenging since the distractors can be with arbitrary variety.

---

[4] A single Canon 7D camera equipped with a Sigma 800mm F5.6 EX APO DG HSM lens.

Table 2: Face verification performance of state-of-the-art FR methods on the LFW challenge. "*": Results from the challenge leaderboard (Huang and Learned-Miller, 2017). M: Million.

Feature Representation	Method	Accuracy (%)	Year	Training IDs	Training Images
Hand Crafted	Joint-Bayes (Chen et al, 2012)	92.42	2012	2,995	99,773
	HD-LBP (Chen et al, 2013)	95.17	2013	2,995	99,773
	TL Joint-Bayes (Cao et al, 2013)	96.33	2013	2,995	99,773
	GaussianFace (Lu and Tang, 2015)	98.52	2015	16,598	845,000
Deep Learning	DeepFace (Taigman et al, 2014)	97.35	2014	4,030	4.18M
	DeepID (Sun et al, 2014c)	97.45	2014	5,436	87,628
	LfS (Yi et al, 2014)	97.73	2014	10,575	494,414
	Fusion (Taigman et al, 2015)	98.37	2015	250,000	7.5M
	VggFace (Parkhi et al, 2015)	98.95	2015	2,622	2.6M
	BaiduFace (Liu et al, 2015a)	99.13	2015	18,000	1.2M
	DeepID2 (Sun et al, 2014a)	99.15	2014	10,177	202,599
	CentreFace (Wen et al, 2016)	99.28	2016	17,189	0.7M
	SphereFace (Liu et al, 2017)	99.42	2017	10,575	494,414
	DeepID2+ (Sun et al, 2015b)	99.47	2015	12,000	290,000
	DeepID3 (Sun et al, 2015a)	99.53	2015	12,000	290,000
	FaceNet (Schroff et al, 2015)	99.63	2015	8M	200M
	TencentYouTu* (Tencent, 2017)	99.80	2017	20,000	2M
	EasenElectron* (Electron, 2017)	99.83	2017	59,000	3.1M

Table 3: The performance summary of state-of-the-art image super-resolution methods on five standard benchmarks. While none of the benchmarks are designed for FR, these evaluations represent a generic capability of contemporary super-resolution techniques in synthesising high frequency details particularly for low-resolution web images. Metric: Peak Signal-to-Noise Ratio (PSNR), higher is better.

Model	Unscalling Times	Set5	Set14	B100	URGAN	MANGA
Bicubic	2	33.65	30.34	29.56	26.88	30.84
SRCNN (Dong et al, 2014)	2	36.65	32.29	31.36	29.52	35.72
FSRCNN (Dong et al, 2016)	2	36.99	32.73	31.51	29.87	36.62
VDSR (Kim et al, 2016a)	2	37.53	33.03	31.90	30.76	-
DRCN (Kim et al, 2016b)	2	37.63	32.98	31.85	30.76	37.57
LapSRN (Lai et al, 2017)	2	37.52	33.08	31.80	30.41	37.27
DRRN (Tai et al, 2017)	2	37.74	33.23	32.05	31.23	-
Bicubic	4	28.42	26.10	25.96	23.15	24.92
SRCNN (Dong et al, 2014)	4	30.49	27.61	26.91	24.53	27.66
FSRCNN (Dong et al, 2016)	4	30.71	27.70	26.97	24.61	27.89
VDSR (Kim et al, 2016a)	4	31.35	28.01	27.29	25.18	-
DRCN (Kim et al, 2016b)	4	31.53	28.04	27.24	25.14	28.97
LapSRN (Lai et al, 2017)	4	31.54	28.19	27.32	25.21	29.09
DRRN (Tai et al, 2017)	4	31.68	28.21	27.38	25.44	-
Bicubic	8	24.39	23.19	23.67	20.74	21.47
SRCNN (Dong et al, 2014)	8	25.33	23.85	24.13	21.29	22.37
FSRCNN (Dong et al, 2016)	8	25.41	23.93	24.21	21.32	22.39
LapSRN (Lai et al, 2017)	8	26.14	24.44	24.54	21.81	23.39

(III) Low-Resolution Face Recognition. A unique FR challenge in surveillance FR is low-resolution (Wang et al, 2014b). For FR on image pairs with large resolution difference, the resolution discrepancy problem emerges. Generally, existing low-resolution FR methods are fallen into two categories: **(1)** image super-resolution (Bilgazyev et al, 2011, Fookes et al, 2012, Gunturk et al, 2003, Hennings-Yeomans et al, 2008, Jia and Gong, 2005, Jiang et al, 2016, Li et al, 2008, Liu et al, 2005, Wang et al, 2016b, Xu et al, 2013, Zou and Yuen, 2012), and **(2)** resolution-invariant learning (Abiantun et al, 2006, Ahonen et al, 2008, Biswas et al, 2010, 2012, Choi et al, 2008, 2009, He et al, 2005, Lei et al, 2011, Li et al, 2009, 2010, Ren et al, 2012, Shekhar et al, 2011, Wang and Miao, 2008, Zhou et al, 2011).

The first category is based on two learning criteria: pixel-level visual fidelity and face ID discrimination. Existing methods often conduct two training processes with more focus on appearance enhancement (Gunturk et al, 2003, Wang and Tang, 2003). There are recent attempts (Hennings-Yeomans et al, 2008, Wang et al, 2016b, Zou and Yuen, 2012) that unite the two subtasks for more discriminative learning.

The second category of methods aims to extract resolution-invariant features (Ahonen et al, 2008, Choi et al, 2009, Lei et al, 2011, Wang and Miao, 2008)

or learning a cross-resolution structure transformation (Choi et al, 2008, He et al, 2005, Ren et al, 2012, Shekhar et al, 2011, Wong et al, 2010). As deep FR models are data driven, they can be conceptually categorised into this strategy whenever suitable training data is available to model optimisation.

However, all the existing methods have a number of limitations: (1) Considering small scale and/or down-sampled artificial low-resolution face images in the closed-set setting, therefore unable to reflect the genuine surveillance FR challenge at scales. (2) Relying on hand-crafted features and linear/shallow model structures, therefore subject to suboptimal generalisation. (3) Requiring coupled low- and high-resolution image pairs from the same domain for model training, but unavailable in the surveillance scenarios.

In low-resolution (LR) imagery face recognition deployments, two typical operational settings exist. One common setting is LR-to-HR (high-resolution) which aims to match LR probe images against HR gallery images such as passport or other document photos (Bilgazyev et al, 2011, Biswas et al, 2010, 2012, Ren et al, 2012, Shekhar et al, 2011). This is a widely used approach by Law Enforcement Agencies to matching potential candidates against a watch-list. On the other hand, there is another operational setting which requires LR-to-LR imagery face matching when both the probe and the gallery images are LR facial images (Fookes et al, 2012, Gunturk et al, 2003, Wang and Tang, 2003, Wang et al, 2016b, Zou and Yuen, 2012).

Generally, LR-to-LR face recognition occurs in a less stringent deployment setting at larger scales when pre-recorded (in a controlled environment) HR facial images of a watch-list do not exist, nor there is a pre-defined watch-list. In an urban environment, there is no guarantee of controlled access points to record HR facial images of an average person in unconstrained public spaces due to the commonly used wide field of view of CCTV surveillance cameras and long distances between the cameras and people. In large, public space video surveillance data contain a very large number of "joe public" without HR facial images pre-enrolled for face recognition. Video forensic analysis often requires large scale people searching and tracking over distributed and disjoint large spaces by face recognition of *a priori* unknown (not enrolled) persons triggered by a public disturbance, when the only available facial images are from LR CCTV videos. More recently, a rapid emergence of smart shopping, such as the Amazon Go, Alibaba Hema and JD 7Fresh supermarkets, also suggests that any face recognition techniques for individualised customer in-store localisation (track-and-tag) cannot assume unrealistically stringent HR facial imagery enrollment of

every single potential customer if the camera system is to be cost effective.

Image Super-Resolution. Super-resolution methods have been significantly developed thanks to the strong capacity of deep CNN models in regressing the pixel-wise loss between reconstructed and ground-truth images (Dong et al, 2014, 2016, Kim et al, 2016a,b, Lai et al, 2017, Ledig et al, 2016, Tai et al, 2017, Yang et al, 2014, Yu and Porikli, 2016). A performance summary of six state-of-the-art deep models on five benchmarks is given in Table 3. Mostly, FR and super-resolution researches advance independently, with both assuming the availability of large high-resolution training data. In surveillance, high-resolution images are typically unavailable, which in turn resorts the existing methods to transfer learning. When the training and test data distributions are very different, super-resolution becomes extremely challenging due to an extra need for domain adaptation.

As an object-specific super-resolution, face hallucination is dedicated to fidelity restoration of facial appearance (Baker and Kanade, 2000, Cao et al, 2017a, Chakrabarti et al, 2007, Jia and Gong, 2008, Jin and Bouganis, 2015, Liu et al, 2007, Wang and Tang, 2005, Yu and Porikli, 2017, Zhu et al, 2016). A common hallucination approach is transferring high-frequency details and structure information from exemplar high-resolution images. This is typically achieved by mapping low- and high-resolution training pairs. Existing methods require noise-free input images, whilst assuming stringent part detection and dense correspondence alignment. Otherwise, overwhelming artifacts may be introduced. These assumptions significantly limit their usability to low-resolution surveillance data due to the presence of uncontrolled noise and the absence of coupled high-resolution images.

## 3 QMUL-SurvFace Recognition Challenge

3.1 A Native Low-Res Surveillance Face Dataset

To our best knowledge, there is no large native surveillance FR challenge in the public domain. To stimulate the research on this problem, we construct a new large scale benchmark (challenge) by automatically extracting faces of the uncooperative general public appearing in real-world surveillance videos and images. We call this challenge **QMUL-SurvFace**. Unlike most existing FR challenges using either high-quality web or simulated surveillance images captured in controlled conditions therefore *failing* to evaluate the true surveillance FR performance, we explore real-world native surveil-

Table 4: Person re-identification datasets utilised in constructing the *QMUL-SurvFace* challenge.

Person Re-Identification Dataset	IDs	Detected IDs	Bodies	Detected Faces	Nation
Shinpuhkan (Kawanishi et al, 2014)	24	24	22,504	6,883	Japan
WARD (Martinel and Micheloni, 2012)	30	11	1,436	390	Italy
RAiD (Das et al, 2014)	43	43	6,920	3,724	US
CAVIAR4ReID (Cheng et al, 2011)	50	43	1,221	141	Portugal
SARC3D (Baltieri et al, 2011b)	50	49	200	107	Italy
ETHZ (Schwartz and Davis, 2009)	148	110	8,580	2,681	Switzerland
3DPeS (Baltieri et al, 2011a)	192	133	1,012	366	Italy
QMUL-GRID (Loy et al, 2009)	250	242	1,275	287	UK
iLIDS-VID (Wang et al, 2014a)	300	280	43,800	14,181	UK
SDU-VID (Liu et al, 2015b)	300	300	79,058	67,988	China
PRID 450S (Roth et al, 2014)	450	34	900	34	Austria
VIPeR (Gray and Tao, 2008)	632	456	1,264	532	US
CUHK03 (Li et al, 2014)	1,467	1,380	28,192	7,911	China
Market-1501 (Zheng et al, 2015)	1,501	1,429	25,261	9,734	China
Duke4ReID (Gou et al, 2017)	1,852	1,690	46,261	17,575	US
CUHK-SYSU (Xiao et al, 2016)	8,351	6,694	22,724	12,526	China
LPW (Song et al, 2017)	4,584	2,655	590,547	318,447	China
Total	20,224	15,573	881,065	463,507	Multiple

lance imagery data from a combination of 17 person re-identification benchmarks which were collected in different surveillance scenarios across diverse sites and multiple countries (Table 4).
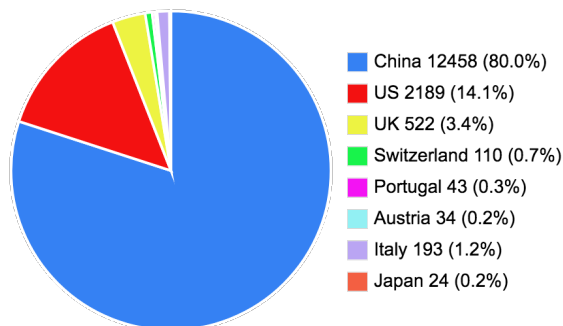
(a) Geographic distribution of face IDs.
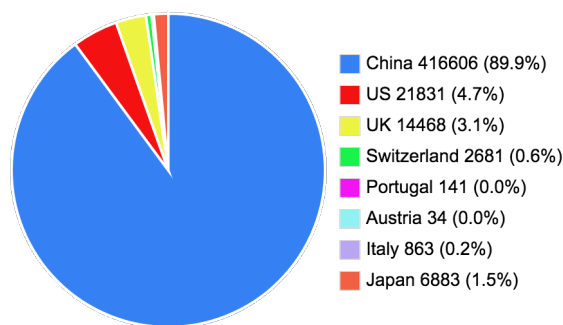
(b) Geographic distribution of face images.

Fig. 2: Geographic distributions of (a) face IDs and (b) face images in the *QMUL-SurvFace* challenge.

Dataset Statistics. The *QMUL-SurvFace* challenge contains 463,507 low-resolution face images of 15,573 unique person IDs with uncontrolled appearance variations in pose, illumination, motion blur, occlusion and background clutter (Fig. 3). Among all, there are 10,638 (68.3%) people each associated with two or more detected face images. This is the largest native surveillance face benchmark to date (Table 1).

Face Image Collection. To enable QMUL-SurvFace represent a scalable test scenario, we automatically extracted the facial images by deploying the TinyFace detector (Hu and Ramanan, 2016) on re-identification surveillance data (Fig. 5). Manually labelling faces is non-scalable due to the huge amount of surveillance video data. Note that not all faces in the source images can be successfully detected given imperfect detection, poor image quality, and extreme head poses. The average face detection recall is 77.0% (15,573 out of 20,224) in ID and 52.6% (463,507 out of 881,065) in image. Face detection statistics across all person re-identification datasets are summarised in Table 4.

Face Image Cleaning and Annotation. To make an accurate FR challenge, we manually cleaned QMUL-SurvFace data by filtering out false detections. We manually thrown away all movie and TV program (non-surveillance) image data in the CUHK-SYSU dataset These were labelled by two independent annotators and a subsequent mutual cross-check. For face ID annotation, we used the person labels available in sources where we assume no ID overlap across datasets. This is rational since they were independently created over different time and surveillance venues, that is, the possibil-

Table 5: Benchmark data partition of *QMUL-SurvFace*. Numbers in parentheses: per-identity image size range.

Split	All	Training	Test
IDs	15,573	5,319	10,254
Images	463,507 (1∼558)	220,890 (2∼558)	242,617 (1∼482)

ity that a person appearing in multiple re-identification datasets is extremely low.

Face Characteristics. In contrast to existing FR challenges, QMUL-SurvFace is uniquely characterised by very low resolution faces typical in video surveillance (Fig. 6) – one major source that makes surveillance FR challenging (Wang et al, 2014b). The face spatial resolution ranges from 6/5 to 124/106 pixels in height/width, and the average is 24/20. This dataset exhibits a power-law distribution in frequency ranging from 1 to 558 (Fig. 7). Besides, the QMUL-SurvFace people feature a wide variation in geographic origin[5] (Fig. 2). Given low-resolution facial appearance, surveillance FR may be less sensitive to the nationality than high-resolution web FR.

3.2 Evaluation Protocols

FR performance are typically evaluated with two applications (verification and identification) and two protocols (closed-set and open-set).

Data Partition. To benchmark the evaluation protocol, we first need to split the *QMUL-SurvFace* data into training and test sets. We divide the 10,638 IDs each with ≥ 2 face images into two halves: one half (5,319) for training, one half (5,319) plus the remaining 4,935 single-shot IDs (in total 10,254) for test (Table 5). We benchmark only *one* train/test data split since the dataset is sufficiently large in ID classes and face images to support a statistically stable evaluation.

We apply the same data partition as above for both face identification and verification. All face images of training IDs are used to train FR models. Additional imagery from other sources may be used subject to no facial images of test IDs. The use of test data depends on the application and protocol. Next, we present the approach for benchmarking *face identification* and *face verification* on QMUL-SurvFace.

Face Verification. The verification protocol measures the comparing performance of face pairs. Most FR methods evaluated on LFW adopt this protocol. Specifically, one presents a face image to a FR system with a claimed

Table 6: Benchmark face verification and identification protocols on *QMUL-SurvFace*. TAR: True Accept Rate; FAR: False Accept Rate; ROC: Receiver Operating Characteristic; FPIR: False Positive Identification Rate; TPIR: True Positive Identification Rate.

1:1 Face Verification Protocol			
Matched Pairs	5,319	Unmatched Pairs	5,319
Metrics	TAR@FAR, ROC		
1:N Face Identification Protocol			
Scenario	Open-Set		
Partition	Probe	Gallery	
IDs	10,254	3,000	
Images	182,323	60,294	
Metrics	TPIR@FPIR, ROC		

ID represented by an enrolled face. The system accepts the claim if their matching similarity score is greater than a threshold t, or rejects otherwise (Phillips et al, 2010). The protocol specifies the sets of *matched* and *unmatched* pairs that FR methods should perform in evaluation. For each test ID, we generate one matched pair, i.e. a total of 5,319 pairs (Table 6). We generate the same number (5,319) of unmatched pairs by randomly sampling between a face and nonmated ones. For performance measurement, each of these pairs is to be evaluated by computing a matching similarity score.

In the verification process, two types of error can occur: (1) A false accept – a distractor claims an ID of interest; (2) A false reject – the system mistakenly declines the ID of interest. As such, we define the False Accept Rate (FAR) as the fraction of unmatched pairs with the corresponding score s above threshold t

$$\text{FAR}(t) = \frac{|\{s \geq t, \text{ where } s \in U\}|}{|U|} \qquad (1)$$

where U denotes the set of unmatched pairs. In contrast, the False Rejection Rate (FRR) represents the fraction of matched pairs with matching score s below a threshold t:

$$\text{FRR}(t) = \frac{|\{s < t, \text{ where } s \in M\}|}{|M|} \qquad (2)$$

where M is the set of matched pairs. For understanding convenience, we further define the True Accept Rate (TAR), the complement of FRR, as

$$\text{TAR}(t) = 1 - \text{FRR}(t). \qquad (3)$$

For face verification evaluation on QMUL-SurvFace, we use the paired TAR@FAR measure.

We also utilise the receiver operating characteristic (ROC) analysis measurement by varying the threshold t and generating a TAR-vs-FAR ROC curve. The overall accuracy performance can be measured by the area

---

[5] In computing the nationality statistics, it is assumed that all people of a person re-identification dataset share the same nationality. Per-ID nationality labels are not available.
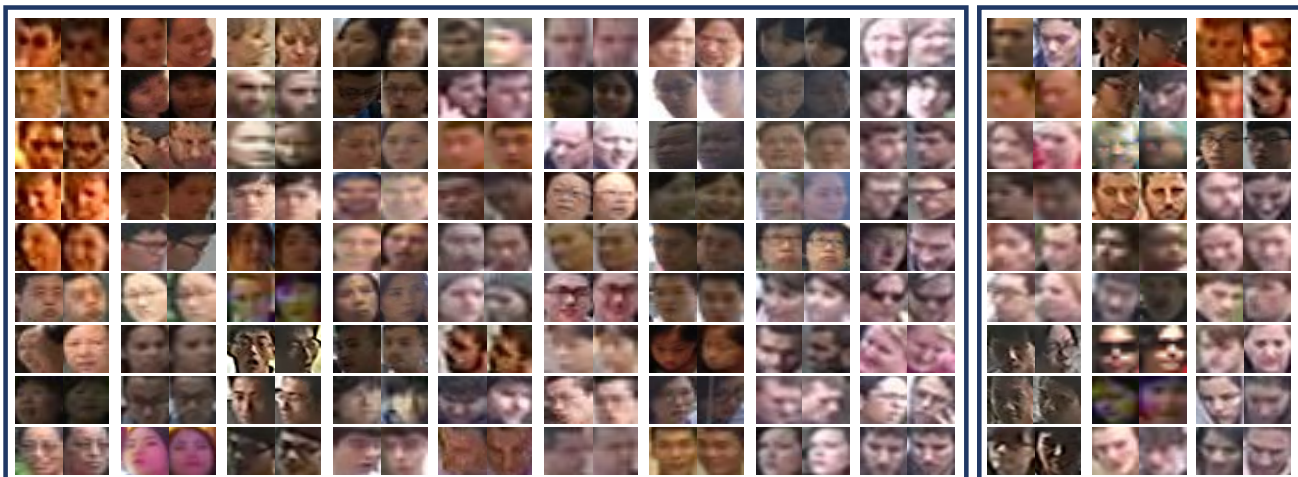
Fig. 3: Example face image pairs from *QMUL-SurvFace*. **Left**: matched pairs. **Right**: unmatched pairs.

under the ROC curve, which is abbreviated as AUC. See the top half of Table 6 for the verification protocol summary.

Face Identification. In forensic and surveillance applications however, it is face identification that is of more interest (Best-Rowden et al, 2014, Ortiz and Becker, 2014), and arguably a more intricate and non-trivial problem since a probe image must be compared against all gallery IDs (K-S et al, 2016, Wang et al, 2016a).

Most existing FR methods in the literature consider the *closed-set* scenario, assuming that each probe subject is present in the gallery. We construct the evaluation setup for the closed-set scenario on QMUL-SurvFace through the following process. For each of the 5,319 multi-shot test IDs, we randomly sample the corresponding images into probe or gallery. The gallery set represents imagery involved in an operational database, e.g. access control system's repository. For any unique person, we generate a single ID-specific face template from one or multiple gallery images (Klare et al, 2015). This makes the ranking list concise and more efficient for post-rank manual validation, e.g. no case that a single ID takes multiple ranks. The probe set represents imagery used to query a face identification system.

For performance evaluation in *closed-set* identification, we select the Cumulative Matching Characteristic (CMC) (Klare et al, 2015) measure. CMC reports the fraction of searches returning the mate (true match) at rank r or better, with the rank-1 rate as the most common summary indicator of an algorithm's efficacy. It is a non-threshold rank based metric. Formally, the CMC at rank r is defined as:

$$\text{CMC}(r) = \sum_{i=1}^{r} \frac{N_{\text{mate}}(i)}{N} \tag{4}$$

where $N_{\text{mate}}(i)$ denotes the number of probe images with the mate ranked at position i, and N the total probe number.

In realistic surveillance applications, however, most faces captured by CCTV cameras are not of any gallery person therefore should be detected as unknown, leading to the *open-set* protocol (Grother and Ngan, 2014, Liao et al, 2014). This is often referred to the *watch-list identification* (forensic search) scenario where only persons of interest are enrolled into the gallery, typically each ID with several different images such as the FBIs most wanted list[6]. To allow for the *open-set* surveillance FR test, we construct a watch list identification protocol where only face IDs of interest are enrolled in the gallery. specifically, we create the following probe and gallery sets: (1) Out of the 5,319 multi-shot test IDs, we randomly select 3,000 and sample half face images for each selected ID into the gallery set, i.e. the watch list. (2) All the remaining images including these single-shot ID imagery are used to form the probe set. As such, the majority of probe people are *unknown* (not enrolled gallery IDs), more accurately reflecting the open space forensic search nature.

For the *open-set* FR performance evaluation, we must quantify two error types (Grother and Ngan, 2014). The first type is *false alarm* – a face image from an unknown person (i.e. nonmate search) is incorrectly associated with one or more enrollees' data. This error is quantified by the *False Positive Identification Rate* (FPIR):

$$\text{FPIR}(t) = \frac{N_{\text{nm}}^{\text{m}}}{N_{\text{nm}}} \tag{5}$$

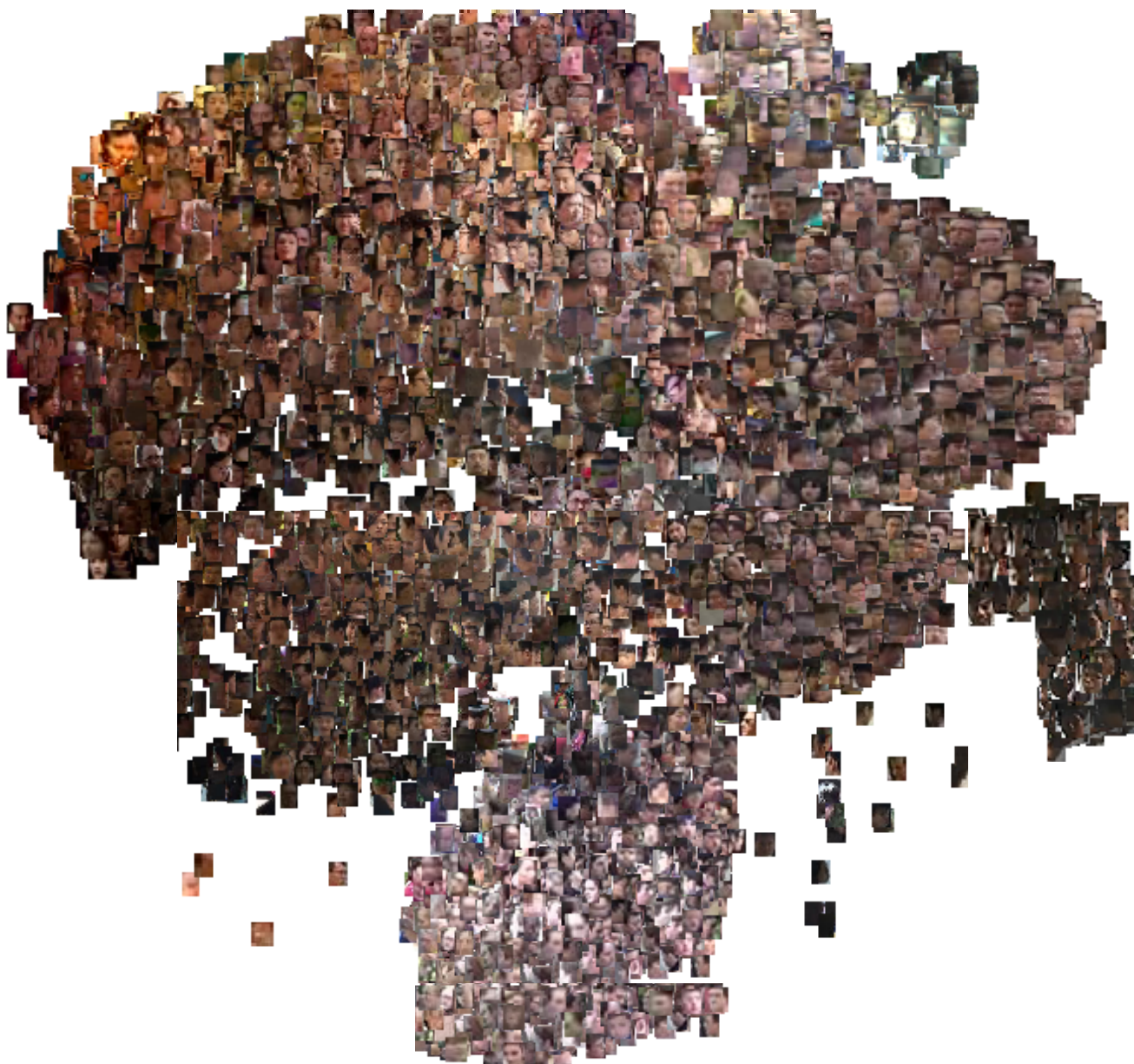
[6] www.fbi.gov/wanted

Fig. 4: A glimpse of native surveillance face images from the *QMUL-SurvFace* challenge.

Fig. 5: Illustration of face detections in native surveillance person images. **Left**: Auto-detected faces. **Right**: Failure cases, the detector fails to identify the face due to low-resolution, motion blur, extreme pose, poor illumination, and background clutters.
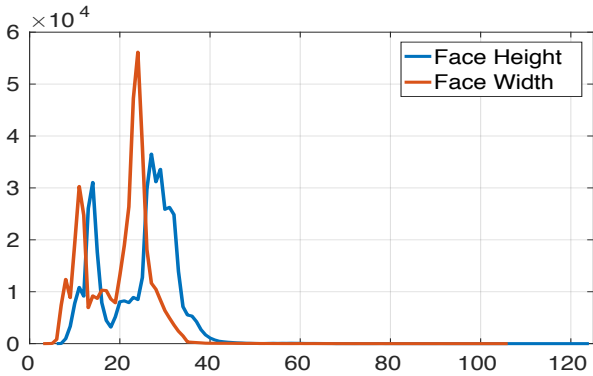
Fig. 6: Scale distributions of *QMUL-SurvFace* images.

Fig. 7: Image frequency over all *QMUL-SurvFace* IDs.

which measures the proportion of nonmate searches N_{nm}^m (i.e. no mate faces in the gallery) that produce one or more enrolled candidates at or above a threshold t (i.e. false alarm), among a total of N_{nm} nonmate searches attempted.

The second type of error is *miss* – a search of an enrolled target persons data (i.e. mate search) does not return the correct ID. We quantify the miss error by the *False Negative Identification Rate* (FNIR):

$$\text{FNIR}(t,r) = \frac{N_m^{nm}}{N_m} \qquad (6)$$

which is the proportion of mate searches N_m^{nm} (i.e. with mate faces present in the gallery) with enrolled mate found outside top r ranks or matching similarity score below the threshold t, among N_m mate searches. By default, we set $r = 20$ (i.e. FNIR$(t, 20)$) which assumes a small workload by a human reviewer employed to review the candidates returned from an identification search (Grother and Ngan, 2014). In practice, a more intuitive measure may be the "hit rate" or *True Positive Identification Rate* (TPIR):

$$\text{TPIR}(t,r) = 1 - \text{FNIR}(t,r) \qquad (7)$$

which is the complement of FNIR offering a positive statement of how often mated searches are succeeded. In QMUL-SurvFace, we adopt the TPIR@FPIR measure as the open-set face identification performance metrics. TPIR-vs-FPIR can similarly generate an ROC curve, the AUC of which stands for an overall measurement (see the bottom half of Table 6).

Link of open-set and closed-set. The aforementioned performance metrics of closed-set and open-set FR are not completely independent but correlated. The CMC(r) (Eqn. (4)) can be regarded as a special case of TPIR(t, r) (Eqn. (7)) with ignored similarity scores by relaxing the threshold requirement t as:

$$\text{CMC}(r) = \text{TPIR}(t,r) \qquad (8)$$

This metrics linkage is useful in enabling performance comparisons between closed-set and open-set.

Considerations. In the literature, existing FR challenges adopt the closed-set evaluation protocol including MegaFace (K-S et al, 2016). While being able to evaluate FR model generalisation capability in large scale search (e.g. 1 million gallery images in MegaFace), it does not fully confirm to the surveillance FR operation. For surveillance FR, human operators are often assigned with a list of target people for a mission with their face images enrolled in a working system. The FR task is then to search the targets in public spaces against the gallery face images. This is an open-set FR problem. As a consequence, we adopt the open-set identification protocol as the main setting of QMUL-SurvFace (Table 6). Besides, we still consider closed-set FR experiments to enable like-for-like comparisons with existing benchmarks.

4 Benchmark Evaluation

In this section, we describe two categories of techniques used in the benchmark evaluations: deep learning FR and image super-resolution methods.

4.1 Face Recognition Models

We present the formulation details of five representative FR models (Table 2): DeepID2 (Sun et al, 2014a), CentreFace (Wen et al, 2016), FaceNet (Schroff et al, 2015), VggFace (Parkhi et al, 2015), and SphereFace (Liu et al, 2017). All the methods are based on CNN architecture each with different objective loss function and network designs. They are designed for learning a discriminative face representation space by increasing inter-ID variations whilst decreasing intra-ID variations. Both variations are intrinsically complex and highly non-linear

due to that faces of the same ID may appear very differently in varying conditions whereas faces of different IDs may look alike. Once a deep FR model is trained by a standard SGD algorithm (Bottou, 2010, Rumelhart et al, 1988), we deploy it as a feature extractor and perform FR with L_2 distance.

The **DeepID2** model (Sun et al, 2014a) is characterised by simultaneously learning face identification and verification supervision. Identification is to classify a face image into one ID class by softmax cross-entropy loss (Krizhevsky et al, 2012). Formally, we predict the posterior probability $\tilde{y}_i$ of a face image $\boldsymbol{I}_i$ over the ground-truth ID class y_i among a total n_{id} distinct training IDs:

$$p(\tilde{y}_i = y_i | \boldsymbol{I}_i) = \frac{\exp(\boldsymbol{w}_{y_i}^\top \boldsymbol{x}_i)}{\sum_{k=1}^{|n_{\mathrm{id}}|} \exp(\boldsymbol{w}_k^\top \boldsymbol{x}_i)} \tag{9}$$

where $\boldsymbol{x}_i$ specifies the DeepID2 feature vector of $\boldsymbol{I}_i$, and $\boldsymbol{W}_k$ the prediction parameter of the k-th ID class. The identification training loss is defined as:

$$l_{\mathrm{id}} = -\log\left(p(\tilde{y}_i = y_i | \boldsymbol{I}_i)\right) \tag{10}$$

The verification signal encourages the DeepID2 features extracted from the same-ID face images to be similar so to reduce the intra-person variations. This is achieved by the pairwise contrastive loss (Hadsell et al, 2006):

$$l_{\mathrm{ve}} = \begin{cases} \frac{1}{2}\|\boldsymbol{x}_i - \boldsymbol{x}_j\|_2^2 & \text{if same ID,} \\ \frac{1}{2}\max\left(0, m - \|\boldsymbol{x}_i - \boldsymbol{x}_j\|_2^2\right)^2 & \text{otherwise.} \end{cases} \tag{11}$$

where m represents the discriminative ID class margin. The final DeepID2 model loss function is a weighted summation of the above two as:

$$\mathcal{L}_{\mathrm{DeepID2}} = l_{\mathrm{id}} + \lambda_{\mathrm{bln}} l_{\mathrm{ve}} \tag{12}$$

where λ_{bln} represents the balancing hyper-parameter. A customised 5-layers CNN is used in the DeepID2.

The **CentreFace** model (Wen et al, 2016) also adopts the softmax cross-entropy loss function (Eqn. (10)) to learn inter-class discrimination. However, it seeks for intra-ID compactness in a class-wise manner by posing a representation constraint that all face image features be close to the corresponding ID centre as possible. Learning this class compactness is accomplished by a centre loss function defined as:

$$l_{\mathrm{centre}} = \frac{1}{2}\|\boldsymbol{x}_i - \boldsymbol{c}_{y_i}\|_2^2 \tag{13}$$

where y_i denotes the ID class of face images $\boldsymbol{x}_i$ and $\boldsymbol{c}_{y_i}$ the up-to-date feature centre of the class y_i. As such, all face images of the same ID are constrained to group

together so that the intra-person variations can be suppressed. The final loss function is integrated with the identification supervision as:

$$\mathcal{L}_{\mathrm{CentreFace}} = l_{\mathrm{id}} + \lambda_{\mathrm{bln}} l_{\mathrm{centre}} \tag{14}$$

Since the feature space is dynamic in the course of training, all class centres are progressively undated on-the-fly. The CentreFace model is implemented in a 28-layers ResNet architecture (He et al, 2016).

The **FaceNet** model (Schroff et al, 2015) sues a triplet loss function (Liu et al, 2009) to learn a binary-class (positive *vs* negative pairs) feature embedding. The triplet loss is to induce a discriminative margin between positive and negative pairs, defined as:

$$\begin{aligned} l_{\mathrm{tri}} = \max\left\{0, \ \alpha - \|\boldsymbol{x}_a - \boldsymbol{x}_n\|_2^2 + \|\boldsymbol{x}_a - \boldsymbol{x}_p\|_2^2\right\}, \\ subject\ to:\ (\boldsymbol{x}_a, \boldsymbol{x}_p, \boldsymbol{x}_n) \in \mathcal{T} \end{aligned} \tag{15}$$

where $\mathcal{T}$ denotes the set of triplets generated based on ID labels, and α is a pre-fixed margin for separating positive ($\boldsymbol{x}_a$, $\boldsymbol{x}_p$) and negative ($\boldsymbol{x}_a$, $\boldsymbol{x}_n$) training pairs. By doing so, the face images for one training ID are constrained to populate on an isolated manifold against other IDs by a certain distance therefore posing a discrimination capability. For fast convergence, it is critical to use triplets that violate the triplet constraint (Eqn. (15)). To achieve this in a scalable manner, we select hard positives and negatives within a mini-batch. In our FaceNet implementation, an Inception-ResNet CNN architecture (Szegedy et al, 2017) is used as a stronger replacement of the originally adopted ZF CNN (Zeiler and Fergus, 2014).

The **VggFace** model (Parkhi et al, 2015) considers both identification and triplet training schemes in a sequential manner. Specifically, we first train the model by a softmax cross-entropy loss (Eqn. (10)). We then learn the feature embedding by a triplet loss (Eqn. (15)) where only the last full-connected layer is updated to implement a discriminative projection. A similar hard sample mining strategy is applied in the second step for more efficient optimisation. The VggFace adopts a 16-layers VGG16 CNN (Simonyan and Zisserman, 2015).

The **SphereFace** model (Liu et al, 2017) exploits a newly designed angular margin based softmax loss function. This loss differs from Euclidean distance based triplet loss (Eqn. (15)) by performing feature discrimination learning in a hyper-sphere manifold. The motivation is that, multi-class features learned by the identification loss exhibit an intrinsic angular distribution.

Formally, the angular softmax loss is formulated as:

$$l_{\mathrm{ang}} = -\log\left(\frac{e^{\|\boldsymbol{x}_i\|\psi(\theta_{y_i},i)}}{e^{\|\boldsymbol{x}_i\|\psi(\theta_{y_i},i)} + \sum_{j \neq y_i} e^{\|\boldsymbol{x}_i\|\psi(\theta_j,i)}}\right),$$

$$\text{where } \psi(\theta_{y_i}, i) = (-1)^k \cos(m\theta_{y_i}, i) - 2k, \quad (16)$$

$$\text{subject to: } \theta_{y_i,i} \in [\frac{k\pi}{m}, \frac{(k+1)\pi}{m}], \quad k \in [0, m-1]$$

where $\theta_{j,i}$ specifies the angle between normalised identification weight $\boldsymbol{W}_j$ ($\|\boldsymbol{W}_j\| = 1$) for j-th class and training sample $\boldsymbol{x}_i$, m ($m \geq 2$) the pre-set angular margin, and y_i the ground-truth class of $\boldsymbol{x}_i$. Specifically, this design manipulates the angular decision boundaries between classes and enforces a constraint $\cos(m\theta_{y_i}) > \cos(\theta_j)$ for any $j \neq y_i$. When $m \geq 2$ and $\theta_{y_i} \in [0, \frac{\pi}{m}]$, this inequation $\cos(\theta_{y_i}) > \cos(m\theta_{y_i})$ holds. Therefore, $\cos(m\theta_{y_i})$ represents a lower boundary of $\cos(\theta_{y_i})$ with larger m leading to a wider angular inter-class margin. Similar to CentreFace, a 28-layers ResNet CNN is adopted in the SphereFace implementation.

4.2 Image Super-Resolution Models

We present the formulation details of five image super-resolution methods (Table 3): SRCNN (Dong et al, 2014), FSRCNN (Dong et al, 2016), LapSRN (Lai et al, 2017), VDSR (Kim et al, 2016a), and DRRN (Tai et al, 2017). Similar to FR methods above, these super-resolution models exploit CNN architectures. A super-resolution model aims to learn a highly non-linear mapping between low- and high-resolution images. This requires ground-truth low- and high-resolution training pairs. Once a model is trained, we deploy it to restore poor resolution surveillance faces before performing FR.

The **SRCNN** model (Dong et al, 2014) is one of the first deep methods achieving remarkable success in super-resolution. The design is motivated by earlier sparse-coding based methods (Kim and Kwon, 2010, Yang et al, 2010). By taking the end-to-end learning advantage of neural networks, SRCNN formulates originally separated components in a unified framework to realise a better mapping function learning. A mean squared error (MSE) is adopted as the loss function:

$$l_{\mathrm{mse}} = \|f(\boldsymbol{I}^{\mathrm{lr}}; \boldsymbol{\theta}) - \boldsymbol{I}^{\mathrm{hr}}\|_2^2 \qquad (17)$$

where $\boldsymbol{I}^{\mathrm{lr}}$ and $\boldsymbol{I}^{\mathrm{hr}}$ denotes coupled low- and high-resolution training images, and $f()$ the to-be-learned super-resolution function with the parameters denoted by $\boldsymbol{\theta}$. This model takes bicubic interpolated images as input.

The **FSRCNN** model (Dong et al, 2016) is an accelerated and more accurate variant of SRCNN (Dong

et al, 2014). This is achieved by taking the original low-resolution images as input, designing a deeper hourglass (shrinking-then-expanding) shaped non-linear mapping module, and adopting a deconvolutional layer for upscaling the input. The MSR loss function (Eqn. (17)) is used for training.

The **VDSR** model (Kim et al, 2016a) improves over SRCNN (Dong et al, 2014) by raising the network depth from 3 to 20 convolutional layers. The rational of deeper cascaded network design is to exploit richer contextual information over large image regions (e.g. 41×41 in pixel) for enhancing high frequency detail inference. To effectively train this model, the residual learning scheme is adopted. That is, the model is optimised to learn a residual image between the input and ground-truth high-resolution images. VDSR is supervised by the MSE loss (Eqn. (17)).

The **DRRN** model (Tai et al, 2017) constructs an even deeper (52-layers) network by jointly exploiting residual and recursive learning. In particular, except for the global residual learning between the input and output as VDSR, this method also exploits local residual learning via short-distance ID branches to mitigate the information loss across all the layers. This leads to a multi-path structured network module. Inspired by (Tai et al, 2017), all modules share the parameters and input so that multiple recursions can be performed in an iterative fashion without increasing the model parameter size. The MSE loss function (Eqn. (17)) is used to supervise in model training.

The **LapSRN** model (Lai et al, 2017) consists in a multi-levels of cascaded sub-networks designed to progressively predict high-resolution reconstructions in a coarse-to-fine fashion. This scheme is hence contrary to the four one-step reconstruction models above. Same as VDSR and DRRN, the residual learning scheme is exploited along with an upscaling mapping function to alleviate the training difficulty whilst enjoying more discriminative learning. For training, it adopts a Charbonnier penalty function (Bruhn et al, 2005):

$$l_{\mathrm{cpf}} = \sqrt{\|f(\boldsymbol{I}^{\mathrm{lr}}; \boldsymbol{\theta}) - \boldsymbol{I}^{\mathrm{hr}}\|_2^2 + \varepsilon^2} \qquad (18)$$

where ε (e.g. set to 10^{-3}) is a pre-fixed noise constant. Compared to MST, this loss has a better potential to suppress training outliers. Each level is supervised concurrently with a separate loss against the corresponding ground-truth high-resolution images. This multi-loss structure resembles the benefits of deeply-supervised models (Lee et al, 2015, Xie and Tu, 2015).

Discussion. It is worth pointing out that using the MSE loss to train a super-resolution model favours the Peak Single-to-Noise Ratio (PSNR) rate, a common

performance measurement. This suits deep neural networks as MSE is differentiable, but cannot guarantee the perceptual quality. One phenomenon is that super-resolved images by an MSE supervised model are likely to be overly-smoothed and blurred. We will evaluate the super-resolution models (Sec. 5.2).

5 Experimental Results

In this section, we present and discuss the experimental evaluations of surveillance FR. The performances of varying FR methods are evaluated on both native low-resolution surveillance faces (Sec. 5.1) and super-resolved faces (Sec. 5.2).

5.1 Low-Resolution Surveillance Face Recognition

We evaluated the FR performance on the *native* low-resolution QMUL-SurvFace images with ambiguous observation. Apart from the low-resolution issue, there are other uncontrolled covariates and noises, e.g. illumination variations, expression, occlusions, background clutter, and compression artifacts. All of these factors cause inference uncertainty to varying degrees (Fig. 3).

Model Training and Test. For training a FR model, we adopted three strategies as below: **(1)** Only using QMUL-SurvFace training set (220,890 images from 5,319 IDs). **(2)** Only using CASIA web data (494,414 images from 10,575 IDs). We will test the effect of using different web source datasets such as MegaFace2 (Nech and K-S, 2017) and MS-Celeb-1M (Guo et al, 2016b). **(3)** First pre-training a FR model on CASIA, then fine-tuning on QMUL-SurvFace. By default we adopt this training strategy. After a FR model is trained by any strategy as above, we deploy it with Euclidean distance.

In both training and test, we rescaled all facial images by *bicubic* interpolation to the required size of a FR model. Such interpolated images are still of "low-resolution" since the underlying resolution is mostly unchanged (Fig. 13).

Evaluation Settings. We considered face verification and identification. By default, we adopt the more realistic open-set evaluation for face identification, unless stated otherwise. For open-set test (Sec. 5.1.1), we used TPIR (Eqn. (6)) at varying FPIR rates (Eqn. (5)). The true match ranked in top-r (i.e. $r = 20$ in Eqn. (7)) is considered as success. For face verification test (Sec. 5.1.2), we used TAR (Eqn. (3)) and FAR (Eqn. (1)).

Implementation Details. For CentreFace (Wen et al, 2016), VggFace (Parkhi et al, 2015), and SphereFace (Liu et al, 2017) we used the codes released by the

original authors. For FaceNet (Schroff et al, 2015), we utilised a TensorFlow reimplementation[7]. We reproduced DeepID2 (Sun et al, 2014a). Throughout the experiments, we adopted the suggested parameter setting by the authors if available, or carefully tuned the hyper-parameters by grid search. Data augmentation was applied to QMUL-SurvFace training data, including flipping, Gaussian kernel blurring, colour shift, brightness and contrast adjustment. We excluded cropping and rotation transformation which bring negative influence due to tight face bounding boxes.

5.1.1 Face Identification Evaluation

(I) Benchmark QMUL-SurvFace. We benchmarked face verification on QMUL-SurvFace in Table 7 and Fig. 8. We make four observations: (1) Not all FR models (e.g. VggFace) converge when directly training on QMUL-SurvFace. As opposite, all models are well trained with CASIA data. Whilst the data size of CASIA is larger, we conjugate that the scale is not a key obstacle as QMUL-SurvFace training data should be arguably sufficient for generic deep model training. Instead this may be more due to extreme challenges posed by poor resolution especially when the model requires high-scale inputs like 224×224 by VggFace. This indicates the dramatic differences between native surveillance FR and web FR. (2) The poorest FR results are yielded by the models trained with only CASIA faces. This is expected due to the clear domain gap between CASIA and QMUL-SurvFace (Fig. 9). (3) Most models are notably improved once pre-trained using CASIA faces. This suggests a positive effect of web data by refining model initialisation. (4) CentreFace is the best performer of the five models. This indicates the efficacy of restricting intra-class variation in training for surveillance FR, consistent with web FR (Wen et al, 2016).

(II) Open-Set *vs* Closed-Set. We compared open-set FR with the conventional closed-set setting on QMUL-SurvFace. In closed-set test, we removed all distractors in the test gallery. We evaluated the top-2 FR models, CentreFace and SphereFace. Table 8 suggests that *closed-set FR is clearly easier than the open-set counterpart*. For instance, CentreFace achieves 27.3% TPIR20@FPIR30% in open-set *vs* 61.1% Rank-20 in closed-set. The gap is even larger at lower false alarm rates. This means that when taking into account the attacking of distractors, FR is much harder.

(III) SurvFace *vs* WebFace. We compared surveillance FR with web FR in the closed-set test. We used CentreFace for example. This model achieves Rank-1

---

[7] https://github.com/davidsandberg/facenet

Table 7: Face identification results on *QMUL-SurvFace*. Protocol: Open-Set. Metrics: TPIR20@FPIR ($r=20$) and AUC. "-": No results available due to failure of model convergence.

| Training Data	QMUL-SurvFace					CASIA (Liu et al, 2015c)					CASIA + QMUL-SurvFace				
Metrics	TPIR20(%)@FPIR				AUC (%)	TPIR20(%)@FPIR				AUC (%)	TPIR20(%)@FPIR				AUC (%)
	30%	20%	10%	1%		30%	20%	10%	1%		30%	20%	10%	1%	
DeepID2	12.5	8.1	3.3	0.2	20.8	4.0	2.1	0.8	0.1	7.9	12.8	8.1	3.4	0.8	20.8
CentreFace	**26.2**	**20.0**	**12.2**	**2.8**	**34.6**	5.7	4.4	2.3	0.2	7.6	**27.3**	**21.0**	**13.8**	**3.1**	**37.3**
FaceNet	10.6	7.9	3.6	0.5	18.9	4.0	3.0	0.8	0.1	6.4	12.7	8.1	4.3	1.0	19.8
VggFace	-	-	-	-	-	**6.5**	**4.8**	**2.5**	**0.2**	**9.6**	5.1	2.6	0.8	0.1	14.0
SphereFace	18.8	13.5	7.0	0.7	26.6	5.9	4.2	2.2	1.7	9.0	21.3	15.7	8.3	1.0	28.1
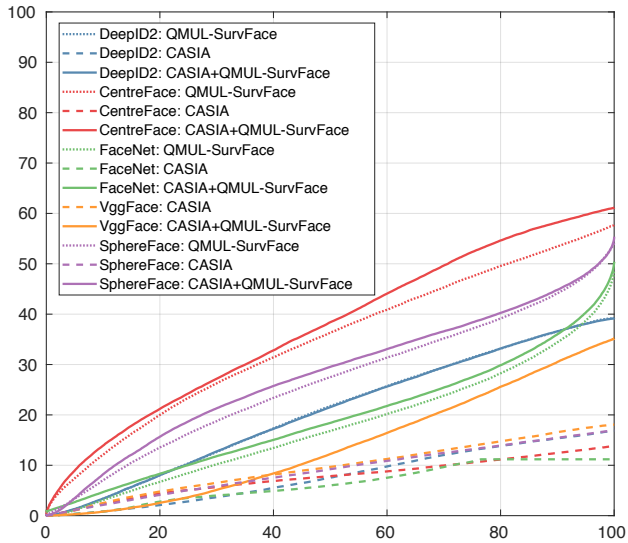
Fig. 8: Face identification results on *QMUL-SurvFace*. Protocol: Open-Set. Metrics: TPIR20@FPIR ($r=20$).

Table 8: Open-Set vs Closed-Set on *QMUL-SurvFace*.

Metrics	TPIR20(%)@FPIR (Open-Set)		
	30%	20%	10%
CentreFace	27.3	21.0	13.8
SphereFace	21.3	15.7	8.3
Metrics	CMC (%) (Closed-Set)		
	Rank-1	Rank-10	Rank-20
CentreFace	29.9	53.4	61.1
SphereFace	29.3	50.0	55.4

29.9% (Table 8) on QMUL-SurvFace, much inferior to the rate of 65.2% on MegaFace, i.e. a 54% (1-29.9/65.2) performance drop. This indicates that surveillance FR is significantly more challenging, especially so when considering that one million distractors are used to additionally complicate the MegaFace test.
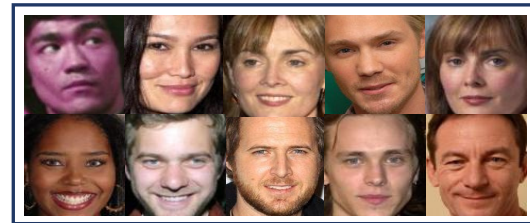
(IV) SurvFace Image Quality. We evaluated the effect of surveillance image quality in open-set FR. To this end, we contrasted QMUL-SurvFace with UCCS (Günther et al, 2017) that provides surveillance face images with clearly better quality (Fig. 9).
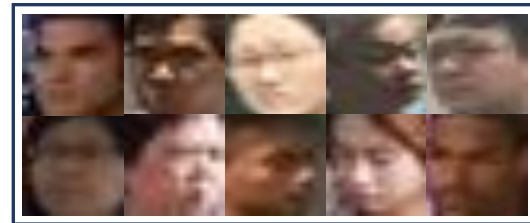
(a) QMUL-SurvFace
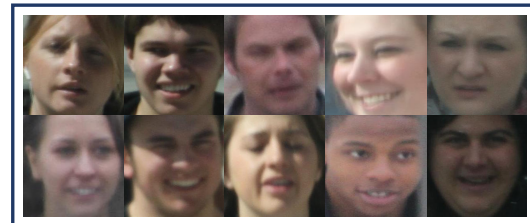
(b) UCCS

(c) CASIA

Fig. 9: Quality comparison of example faces from (a) QMUL-SurvFace, (b) UCCS, and (c) CASIA.

Table 9: Image quality in face identification: UCCS *vs* QMUL-SurvFace(1090ID).

Challenge	Model	TPIR20(%)@FPIR				AUC (%)
		30%	20%	10%	1%	
UCCS	DeepID2	70.7	61.7	48.3	10.0	76.9
	CentreFace	**96.1**	**94.6**	**90.4**	**80.7**	**96.1**
	FaceNet	91.0	89.3	83.6	66.3	91.5
	VggFace	71.0	60.3	46.6	15.0	77.0
	SphereFace	74.0	67.5	58.0	26.8	76.5
QMUL	DeepID2	45.0	34.0	22.0	4.6	55.3
	CentreFace	52.0	46.0	35.0	13.0	60.3
	FaceNet	55.0	49.3	40.5	16.0	59.9
	VggFace	42.0	32.0	21.0	5.0	51.0
	SphereFace	**59.9**	**56.0**	**49.0**	**20.0**	**64.0**

Setting. For UCCS, we used the released face images from 1,090 out of 1,732 IDs with the remaining not accessible. We made a 545/545 train/test ID random split, resulting in a 6,948/7,068 image split. To enable a like-for-like comparison, we constructed a *QMUL-SurvFace(1090ID)* dataset by randomly picking 545/545 QMUL-SurvFace train/test IDs. For evaluation, we designed an open-set test setting using 100 random IDs for gallery and all 545 IDs for probe.

Results. Table 9 shows that QMUL-SurvFace poses more challenges than UCCS, with varying degrees of performance drops experienced by different FR models. This suggests that image quality is an important factor, and UCCS is less accurate in reflecting the surveillance FR challenges due to *artificially* high image quality.

Table 10: LR-to-LR *vs* LR-to-HR FR on UCCS.

Setting	Model	TPIR20(%)@FPIR				AUC (%)
		30%	20%	10%	1%	
LR-to-LR	CentreFace	**92.0**	**90.2**	**87.0**	**70.0**	**93.0**
	FaceNet	89.8	**87.5**	**82.4**	**55.3**	**90.9**
LR-to-HR	CentreFace	91.7	90.1	84.6	66.7	92.8
	FaceNet	89.8	86.6	79.1	50.3	90.1

(V) LR-to-LR *vs* LR-to-HR. We compared the two common low-resolution FR deployment settings on the UCCS benchmark dataset. It is observed in Table 10 that most performances are comparable, suggesting that LR-to-LR and LR-to-HR exhibit similar low-resolution face recognition challenges. Interestingly, LR-to-LR results are relatively better. This is due to less resolution gap to bridge than those of LR-to-HR.

(VI) Test Scalability. We examined the test scalability by comparing QMUL-SurvFace(1090ID) and QMUL-SurvFace. It is shown in the comparison between Table 7 and Table 9 that significantly higher FR performances are yielded on the smaller test with 1090 IDs. This suggests that a large test benchmark is necessary and crucial for enabling the true performance evaluation of practical applications.

(VII) Web Image Resolution. We examined the impact of CASIA web face resolution on surveillance FR. We compared the common 112×96 size with QMUL-SurvFace average resolution 24×20. It is observed in Table 11 that matching web face to QMUL-SurvFace in resolution does not bring performance benefit in most cases. This is because web face images only give limited contribution for surveillance FR due to severe domain discrepancy (Table 7), and simply aligning image resolution cannot alleviate this problem.

Table 11: Effect of web image resolution.

Resolution	Model	TPIR20(%)@FPIR				AUC (%)
		30%	20%	10%	1%	
24×20	DeepID2	12.7	8.1	3.4	0.2	20.6
	CentreFace	27.0	21.0	**14.0**	**3.2**	37.3
	FaceNet	12.3	8.0	4.3	0.5	19.6
	VggFace	5.1	**2.8**	**1.1**	0.1	11.3
	SphereFace	-	-	-	-	-
112×96	DeepID2	**12.8**	8.1	3.4	0.8	**20.8**
	CentreFace	**27.3**	21.0	13.8	3.1	37.3
	FaceNet	**12.7**	**8.1**	4.3	**1.0**	**19.8**
	VggFace	5.1	2.6	0.8	0.1	**14.0**
	SphereFace	**21.3**	**15.7**	**8.3**	**1.0**	**28.1**

Table 12: Selection of web training data source.

| Web Dataset	Model	TPIR20(%)@FPIR				AUC (%)
		30%	20%	10%	1%	
MS-Celeb-1M	CentreFace	**28.0**	**21.9**	14.1	3.1	37.4
	SphereFace	20.1	13.6	5.4	0.8	27.1
MegaFace2	CentreFace	27.7	**21.9**	**15.0**	**3.5**	**37.6**
	SphereFace	20.0	13.0	5.4	0.7	26.4
CASIA	CentreFace	27.3	21.0	13.8	3.1	37.3
	SphereFace	**21.3**	**15.7**	**8.3**	**1.0**	**28.1**

(VIII) Web Image Source. We tested the performance effect of web training dataset by comparing three benchmarks: CASIA (Yi et al, 2014), MS-Celeb-1M (Guo et al, 2016b), and MegaFace2 (Nech and K-S, 2017). We evaluated CentreFace and SphereFace optimised by the suggested training strategies. Table 12 shows that the selection of web data only leads to neglectable changes in surveillance FR performance. For training, CASIA is tens of times more cost-effective (cheaper) than the other two larger datasets, so we use it in the main experiments. Moreover, it is more challenging to train a FR model given a vast ID class space such as MegaFace2.

Table 13: Effect of QMUL-SurvFace image resolution.

Face Width (Pixels)	Model	TPIR20(%)@FPIR				AUC (%)
		30%	20%	10%	1%	
≤20	CentreFace	**32.9**	**23.3**	**15.2**	**4.0**	**40.0**
	SphereFace	13.9	9.4	4.3	0.6	22.4
>20	CentreFace	25.0	19.7	13.5	3.4	34.6
	SphereFace	**26.2**	**21.6**	**14.8**	**2.7**	**32.2**
All	CentreFace	27.3	21.0	13.8	3.1	37.3
	SphereFace	21.3	15.7	8.3	1.0	28.1

(IX) SurvFace Resolution. We examined the effect of test image resolution. Given the bi-modal distribution of QMUL-SurvFace images, we divided all test probe faces into two groups at the threshold of 20 pixels in width and evaluated the FR performance on each group. Table 13 shows that whilst the face dimension matters, the average performance on all test images summarises rather well that of each group. The perfor-

mance variation across groups relies on both FR models applied and other imaging factors, suggesting that the resolution *alone* does not bring a *consistent* performance bias.
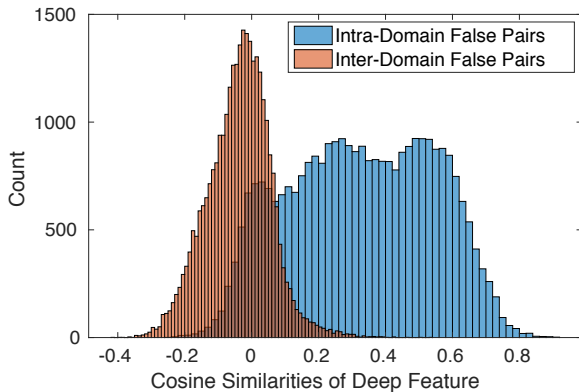
(a) In the *CentreFace* feature space.
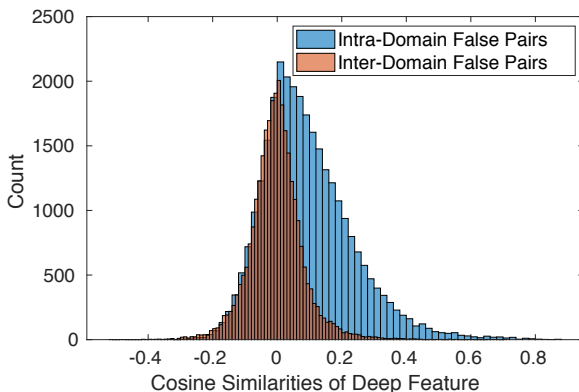
(b) In the *SphereFace* feature space.

Fig. 10: Similarity distributions of *Intra-Domain* and *Inter-Domain* false pairs in the feature space established by (a) CentreFace and (b) SphereFace.

(X) Intra-Domain Similarity Effect. We analysed the intra-domain similarity effect in QMUL-SurvFace – That is, we tested whether face images from one source (domain) are all easily different from other domains. This common domain characteristics may overwhelm the more subtle facial identity differences across domains. To that end, we examined the similarity statistics of *intra-domain* and *inter-domain* false pairs. Specifically, we formed 60,000 intra-domain and 60,000 inter-domain probe-gallery false pairs, and profiled their cosine similarity values measured by the CentreFace and SphereFace features, respectively. Fig. 10 shows that the intra-domain similarity effect is not severe with a large overlap between inter-domain and intra-domain in the matching score (x-axis) range for both CentreFace

and SphereFace. This indicates that different source domains of QMUL-SurvFace do not impose implicitly trivial dominant intra-domain influence, therefore this benchmark does provide a meaningfully challenging open-set test.

(XI) Qualitative Evaluation. To provide a visual evaluation, we show face identification examples by CentreFace on QMUL-SurvFace in Fig. 11. The model succeeds in finding the true match among top-20 in the top three tasks, and fails the last. Poor quality surveillance data present extreme FR challenges.

5.1.2 Face Verification Evaluation

Table 14: Face verification results on *QMUL-SurvFace*.

Model	TAR(%)@FAR				AUC (%)
	30%	10%	1%	0.1%	
DeepID2	80.6	60.0	28.2	13.4	84.1
CentreFace	**95.2**	**86.0**	**53.3**	**26.8**	**94.8**
FaceNet	94.6	79.9	40.3	12.7	93.5
VggFace	83.2	63.0	20.1	4.0	85.0
SphereFace	80.0	63.6	34.1	15.6	83.9

(I) Benchmark QMUL-SurvFace. We benchmarked face verification on QMUL-SurvFace. It is shown in Table 14, that CentreFace remains the best performer as in face identification (Table 7). A divergence is that FaceNet achieves the 2nd position, beating SphereFace. This suggests an operational difference between face identification and verification. All models perform poorly at low FAR (e.g. 0.1%), indicating that face verification in surveillance images is still an unsolved task.

Table 15: Face verification results on *QMUL-SurvFace*.

Model	Mean Accuracy (%)
DeepID2	76.12
CentreFace	**88.00**
FaceNet	85.31
VggFace	77.96
SphereFace	77.57

(II) SurvFace *vs* WebFace. We used LFW (Huang et al, 2007) to compare surveillance and web image based face verification. To this end, we additionally evaluated QMUL-SurvFace by *mean accuracy* (as Table 2), i.e. the fraction of correctly verified pairs. It is seen in Table 15 that the best performance on QMUL-SurvFace is 88.00% by CentreFace, considerably lower than the best LFW result 99.83%. This suggests a higher challenge of FR in surveillance imagery data.

Fig. 11: Face identification examples by CentreFace on *QMUL-SurvFace*. True matches are in red box.

Table 16: Image quality in face verification: UCCS *vs* QMUL-SurvFace(1090ID).

Challenge	Model	TAR(%)@FAR				AUC (%)
		30%	10%	1%	0.1%	
UCCS	DeepID2	93.1	83.4	61.7	37.9	93.8
	CentreFace	**99.6**	**97.0**	**87.8**	**75.5**	**99.0**
	FaceNet	98.2	93.8	79.4	63.4	97.8
	VggFace	97.1	90.6	72.4	55.1	96.7
	SphereFace	94.0	84.9	60.2	24.7	94.1
QMUL	DeepID2	77.3	56.9	24.3	13.1	82.5
	CentreFace	**87.6**	**69.5**	31.1	9.5	**88.5**
	FaceNet	82.9	61.3	29.2	**12.5**	84.6
	VggFace	77.4	54.6	23.4	8.9	82.1
	SphereFace	80.2	62.3	**32.5**	**12.5**	84.1

(III) SurvFace Image Quality. We evaluated the effect of surveillance image quality in face verification by contrasting QMUL-SurvFace(1090ID) and UCCS. We similarly generated 5,319 positive and 5,319 negative test UCCS pairs (Table 6). For a fair comparison, we used only the 7,922 training images of 545 IDs in QMUL-SurvFace(1090ID) for model training. It is evident in Table 16 that the FR performance on UCCS is clearly higher than on QMUL-SurvFace. This is consistent with face identification test (Table 9).

(IV) Qualitative Evaluation. To give visual examination, we show face verification examples by CentreFace at FAR=10% on QMUL-SurvFace in Fig. 12.

5.2 Super-Resolution in Surveillance Face Recognition

Following the FR evaluation in raw low resolution surveillance data, we tested *super-resolved* face images. The aim is to examine the effect of image super-resolution or hallucination techniques in addressing the low-resolution problem in surveillance FR. In this test, we only evaluated the native low-resolution QMUL-SurvFace benchmark, since UCCS images are *artificially* of high resolution therefore excluded (Fig. 9).

(a) Ground-truth: *matched* pairs.

(b) Ground-truth: *unmatched* pairs.

Fig. 12: Face verification examples by CentreFace on *QMUL-SurvFace*. Failure cases are indicated in red.

Model Training and Test. For enhancing deep FR models with image super-resolution capability, we consider two training strategies.

(1) ***Independent Training***: We first pre-train FR models on CASIA (Liu et al, 2015c) and then fine-tune on QMUL-SurvFace, same as in Sec. 5.1. We subsequently *independently* train image super-resolution models with CASIA data alone, since no high-resolution QMUL-SurvFace data are available. Low-res CASIA faces are generated by down-sampling high-resolution ones, which together form training pairs for super-resolution models. In test, we deployed the learned super-resolution models to restore low-resolution QMUL-SurvFace images before performing FR by deep features and Euclidean distance.

(2) ***Joint Training***: Training super-resolution and FR models *jointly* in a hybrid pipeline to improve their

Table 17: Effect of image super-resolution in face identification on *QMUL-SurvFace*. Protocol: Open-Set. SR: Super-Resolution. Jnt/Ind Train: Joint/Independent Training.

Metrics		TPIR20(%)@FPIR				AUC(%)	TPIR20(%)@FPIR				AUC(%)	TPIR20(%)@FPIR				AUC(%)
		30%	20%	10%	1%		30%	20%	10%	1%		30%	20%	10%	1%	
FR Model / SR Model		DeepID2					CentreFace					FaceNet				
No SR		**12.8**	**8.1**	**3.4**	**0.8**	**20.8**	**27.3**	**21.0**	**13.8**	**3.1**	**37.3**	**12.7**	**8.1**	**4.3**	**1.0**	**19.8**
SRCNN	Ind Train	**12.3**	**8.0**	**3.4**	**0.3**	**19.8**	25.0	20.0	**13.1**	3.0	35.0	12.3	8.0	4.1	0.5	19.6
	Jnt Train	6.0	3.7	1.6	0.2	8.5	**25.5**	**20.5**	12.0	2.9	35.0	-	-	-	-	-
FSRCNN	Ind Train	**11.0**	**7.5**	**3.1**	0.1	**19.5**	25.0	**20.0**	12.9	3.0	**35.0**	12.0	7.8	4.0	0.5	19.6
	Jnt Train	8.2	4.9	2.1	**0.2**	15.8	25.0	19.0	11.1	2.9	32.8	-	-	-	-	-
VDSR	Ind Train	**12.2**	**7.0**	**3.3**	0.2	**19.9**	25.5	20.1	**12.8**	3.0	35.1	12.1	7.8	4.0	0.6	19.7
	Jnt Train	9.5	5.7	2.4	**0.3**	18.1	**26.7**	**20.4**	12.6	**3.1**	**35.3**	-	-	-	-	-
DRRN	Ind Train	12.1	7.7	3.2	0.2	19.9	25.5	20.6	12.5	3.0	35.0	12.3	7.9	4.1	0.6	19.5
	Jnt Train	-	-	-	-	-	-	-	-	-	-	-	-	-	-	-
LapSRN	Ind Train	12.0	7.8	3.1	0.2	19.9	25.6	20.0	12.7	3.0	35.1	12.3	7.9	4.1	0.5	19.6
	Jnt Train	-	-	-	-	-	-	-	-	-	-	-	-	-	-	-

FR Model / SR Model		VggFace					SphereFace				
No SR		5.1	2.6	0.8	0.1	14.0	**21.3**	**15.7**	**8.3**	**1.0**	**28.1**
SRCNN	Ind Train	**6.2**	**3.1**	**1.0**	**0.1**	**15.3**	20.0	14.9	6.2	0.6	27.0
	Jnt Train	-	-	-	-	-	-	-	-	-	-
FSRCNN	Ind Train	5.4	2.7	0.8	0.1	14.3	20.0	14.4	6.1	0.7	27.3
	Jnt Train	-	-	-	-	-	-	-	-	-	-
VDSR	Ind Train	5.8	2.9	1.0	0.1	15.0	20.1	14.5	6.1	0.8	27.3
	Jnt Train	-	-	-	-	-	-	-	-	-	-
DRRN	Ind Train	5.8	2.9	0.8	0.1	15.1	20.3	14.9	6.3	0.6	27.5
	Jnt Train	-	-	-	-	-	-	-	-	-	-
LapSRN	Ind Train	5.7	2.8	0.9	0.1	15.0	20.2	14.7	6.3	0.7	27.4
	Jnt Train	-	-	-	-	-	-	-	-	-	-

compatibility. Specifically, we unit super-resolution and FR models by connecting the former's output with the latter's input so allowing an end-to-end training of both. In practice, we first performed joint learning with CASIA and then fine-tuned FR with QMUL-SurvFace. But joint training is not always feasible due to additional challenges such as over-large model size and more challenging to converge the model training. In our experiments, we achieved joint training of six hybrid pipelines among three super-resolution (SRCNN (Dong et al, 2014), FSRCNN (Dong et al, 2016), VDSR (Kim et al, 2016a)) and two FR models (DeepID2 (Sun et al, 2014a) and CentreFace (Wen et al, 2016)). At test time, we deployed the hybrid pipeline on QMUL-SurvFace images to perform FR using Euclidean distance.

Evaluation Settings. For performance metrics, we used TPIR (Eqn. (6)) and FPIR (Eqn. (5)) for face verification and TAR (Eqn. (3)) and FAR (Eqn. (1)) for face identification, same as Sec. 5.1.

Implementation Details. For super-resolution, we performed a 4× upscaling restoration. We used the released codes by the authors for all super-resolution models. In model training, we followed the parameter setting as suggested by the authors if available, or carefully tuned them throughout the experiments.

5.2.1 Face Identification Evaluation

(I) Effect of Super-Resolution. We tested the effect of image super-resolution in surveillance FR on QMUL-SurvFace. From Table 17, we have two observations: (1) Surprisingly, exploiting super-resolution algorithms often bring slightly *negative* effect to surveillance FR. The plausible reasons are threefold. The *first* is due to that the MSE loss (Eqn. (17)) of super-resolution models is not a perceptual measurement, but a low-level pixel-wise metric. The *second* is that the training data for super-resolution are CASIA web faces with a domain gap against QMUL-SurvFace images (Fig. 1). The *third* is the negative effect of artefacts generated in super-resolving (Fig. 13). A slight exception case (similar as in Sec. 5.1) is VggFace due to the need for higher-resolution inputs therefore somewhat preference towards super-resolution. Besides, VggFace is the weakest in performance. (2) Joint training of FR and super-resolution is not necessarily superior than independent training. This suggests that it is non-trivial to effectively propagate the FR discrimination capability into the learning of super-resolution. Therefore, it is worth further in-depth investigation on how to integrate a super-resolution ability with surveillance FR.

Fig. 13: Super-resolved images on QMUL-SurvFace by independently (**left box**) and jointly trained (**right box**) super-resolution models. CentreFace is used in joint training.

Table 18: Effect of super-resolution on down-sampled *MegaFace2* data. Protocol: Open-Set.

Metrics	TPIR20(%)@FPIR				AUC (%)
	30%	20%	10%	1%	
SR \\ FR	CentreFace				
No SR	39.9	28.0	14.0	5.8	46.0
SRCNN	26.6	19.2	10.0	5.0	36.5
FSRCNN	26.3	19.5	11.0	5.2	35.3
VDSR	**40.0**	**28.3**	**14.1**	**6.0**	**47.5**
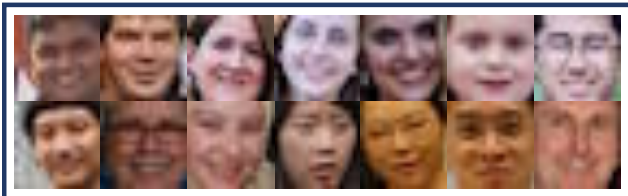
(a) Simulated low-resolution MegaFace2 images.
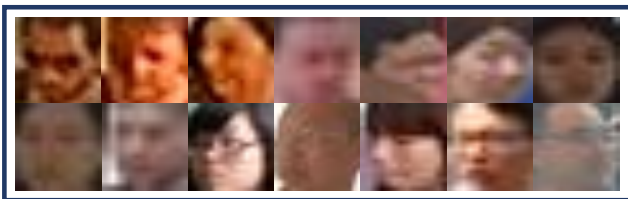
(b) Native low-resolution QMUL-SurvFace.

Fig. 14: Simulated *vs* native low-resolution faces.

(II) SurvFace *vs* WebFace. We evaluated the effect of super-resolution on down-sampled web FR as a comparison to surveillance FR. This mitigates the domain gap between training and test data as encountered on QMUL-SurvFace.

Setting. We constructed a low-resolution web FR dataset with a similar setting as QMUL-SurvFace (Table 5) by
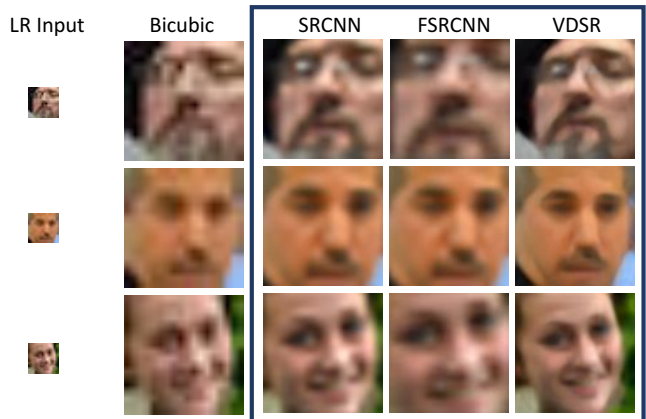
Fig. 15: Super-resolved MegaFace2 images. CentreFace is used jointly with the super-resolution models.

sampling MegaFace2 (Nech and K-S, 2017). MegaFace2 was selected since it contains non-celebrity people thus ensuring ID non-overlap with the training data CASIA. We down-sampled selected MegaFace2 images to the mean QMUL-SurvFace size 24×20 (Fig. 14), and built an open-set test setting with 3,000 gallery IDs (51,949 images) and 10,254 probe IDs (176,990 images) (Table 6). We further randomly sampled an ID-disjoint training set with 81,355 images of 5,319 IDs. In doing so, we created a like-for-like setting with low-resolution MegaFace2 against QMUL-SurvFace. We adopted the most effective joint training strategy.

Results. Table 18 shows that super-resolution at most brings very marginal gain to low-resolution FR performance, suggesting that contemporary techniques are still far from satisfactory in synthesising FR discriminative fidelity (Fig. 15). In comparison, the FR per-

formance assisted by VDSR in particular on simulated low-resolution web faces is better than on surveillance images, similarly reflected in super-resolved images (Fig. 15 vs Fig. 13). This indicates that low-resolution surveillance FR is more challenging due to the lack of high-resolution surveillance data.

Table 19: Effect of super-resolution (SR) in face verification on *QMUL-SurvFace*.

Metrics	TAR(%)@FAR				AUC (%)
	30%	10%	1%	0.1%	
FR / SR	CentreFace (Wen et al, 2016)				
No SR	**95.2**	**86.0**	**53.3**	**26.8**	**94.8**
SRCNN	94.0	82.0	48.1	25.0	93.3
FSRCNN	93.8	81.6	46.0	22.0	93.0
VDSR	95.0	84.0	50.0	26.0	94.5

5.2.2 Face Verification Evaluation

We evaluated the effect of super-resolution for pairwise face verification on QMUL-SurvFace. We used the jointly trained CentreFace model. Table 19 shows that all methods decrease the performance slightly, consistent with the face identification test above (Table 17). Moreover, the verification result is largely unsatisfactory at strict false alarm rates, e.g. FAR=0.1%. Yet, this is very desired for real-world applications because FAR is closely concerned with the system usability. This indicates that there exists a large room for image super-resolution and hallucination towards improving face verification in surveillance facial images.

6 Discussion and Conclusion

In this work, we have presented a large surveillance face recognition benchmark called *QMUL-SurvFace*, including a real-world surveillance face dataset with native low-resolution facial images, extensive benchmarking experimental results, in-depth discussions and analysis. In contrast to existing FR challenges on which the model performances have saturated, this challenge shows that state-of-the-art algorithms remain unsatisfactory in handling poor quality surveillance face images. In concluding remarks, we discuss a number of research directions which we consider to be worthwhile investigating in the future research.

Transfer Learning. From the benchmarking results (Table 17), it is shown that transferring the knowledge of auxiliary web facial data is beneficial to boost the surveillance FR performance. However, more research

is needed to achieve more effective transfer. Given the domain discrepancy between surveillance and web face images, it is important to consider domain adaptation in training (Ganin and Lempitsky, 2015, Ghifary et al, 2016, Pan and Yang, 2010, Saenko et al, 2010, Tzeng et al, 2015). Among existing solutions, style transfer (Gatys et al, 2016, Li and Wand, 2016, Li et al, 2017, Zhu et al, 2017) is a straightforward approach. The idea is to transform the source images with the target domain style so that the labelled source data can be exploited to train supervised FR models. Whilst solving the style transfer problem is inherently challenging, it promises worthwhile potential for surveillance FR.

Resolution Restoration. As mentioned earlier, the low-resolution nature hinders the surveillance FR performance. While image super-resolution (SR) is one natural solution, our evaluations show that the current algorithms are not effective. Two main reasons are: (1) We have no access to native high-resolution surveillance faces required in training SR models (Yang et al, 2014). (2) It is difficult to transfer the SR model learned on web data due to the domain gap (Pan and Yang, 2010). Although SR techniques have been adopted to improve low-resolution FR (Wang et al, 2014b), they rely on hand-crafted feature representations with limited test on small simulated data. It remains unclear how effective SR methods are for native surveillance FR.

Semantic Attributes. Face attributes serve as a mid-level representation to boost FR in high-resolution facial images (Berg and Belhumeur, 2013, Kumar et al, 2009, Manyam et al, 2011, Song et al, 2014). In general, it is challenging to detect attributes in face due to complex covariates in pose, expression, lighting, occlusion, and background (Farhadi et al, 2009, Parikh and Grauman, 2011), besides imbalanced class distributions (Dong et al, 2017, 2018, Huang et al, 2016). And this is even harder given poor quality surveillance images. This direction becomes more plausible due to the emergence of large attribute datasets (Liu et al, 2015c). We anticipate that attributes will play an important role in the development of surveillance FR techniques.

Face Alignment. Face alignment by landmark detection is an indispensable preprocessing in FR (Chen et al, 2012, Wen et al, 2016, Zhang et al, 2016). Despite the great progress (Cao et al, 2014, Zhang et al, 2014, Zhu et al, 2015), aligning face remains a formidable challenge especially in surveillance images (Fig. 16). Similar to SR and attribute detection, this task suffers the domain shift. One idea is hence to construct a large surveillance face landmark dataset. Integrating landmark detection with SR is also an interesting topic.
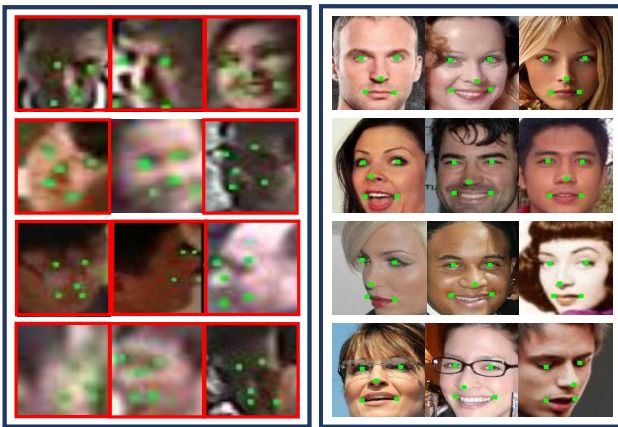
(a) QMUL-SurvFace   (b) CASIA web faces

Fig. 16: Facial landmark detection (Zhang et al, 2016) on randomly sampled (a) QMUL-SurvFace and (b) CA-SIA web faces. Landmarks include left/right eye centres, nose tip, and left/right mouth corners, denoted by green dots. Failure cases are indicated by red box.

Contextual Constraints. Given incomplete and noisy observation in surveillance facial data, it is important to discover and model context information as extra constraint. In social environment, people often travel in groups. The group structure provides useful information (social force) for model inference (Gallagher and Chen, 2009, Helbing and Molnar, 1995, Hughes, 2002, Zheng et al, 2009).

Open-Set Recognition. Surveillance FR is an open-set recognition problem (Bendale and Boult, 2015, 2016). In reality, most probes are non-target persons. It is hence beneficial that the model learn to construct a decision boundary for the target people (Zheng et al, 2016). Whilst open-set recognition techniques evolve independently, we expect more future attempts at jointly solving the two problems.

Zero-Shot Learning. FR is about zero-shot learning (ZSL) with no training samples of test classes available (Fu et al, 2017). In the literature, the focus of ZSL is knowledge transfer across seen and unseen classes via intermediate representations such as attributes (Fu et al, 2014) and word vectors (Frome et al, 2013). All classes are assigned with fixed representations. On the contrary, FR does not use such bridging information but learns an ID-sensitive representation from training classes. In this sense, FR is more generalised.

Imagery Data Scalability. Compared to existing web FR benchmarks (K-S et al, 2016, Liu et al, 2015c, Nech and K-S, 2017, Yi et al, 2014), the QMUL-SurvFace is smaller in scale. An important future effort is to ex-pand this challenge for more effective model training and further scaling up the open-set test.

Final Remark. Given that FR performance has largely saturated on existing web face challenges, this work presents timely a more challenging benchmark QMUL-SurvFace for further stimulating innovative algorithms. This benchmark calls for more research efforts for the under-studied and crucial surveillance FR problem.

Acknowledgements

References

Abate AF, Nappi M, Riccio D, Sabatino G (2007) 2d and 3d face recognition: A survey. Pattern Recognition Letters 28(14):1885–1906

Abiantun R, Savvides M, Kumar BV (2006) How low can you go? low resolution face recognition study using kernel correlation feature analysis on the frgcv2 dataset. In: Symposium on research at the Biometric consortium conference

Adini Y, Moses Y, Ullman S (1997) Face recognition: The problem of compensating for changes in illumination direction. IEEE Transactions on Pattern Analysis and Machine Intelligence 19(7):721–732

Ahonen T, Hadid A, Pietikainen M (2006) Face description with local binary patterns: Application to face recognition. IEEE Transactions on Pattern Analysis and Machine Intelligence 28(12):2037–2041

Ahonen T, Rahtu E, Ojansivu V, Heikkila J (2008) Recognition of blurred faces using local phase quantization. In: IEEE International Conference on Pattern Recognition

Baker S, Kanade T (2000) Hallucinating faces. In: IEEE Conference on Automatic Face and Gesture Recognition

Baltieri D, Vezzani R, Cucchiara R (2011a) 3dpes: 3d people dataset for surveillance and forensics. In: ACM workshop on Human Gesture and Behavior Understanding

Baltieri D, Vezzani R, Cucchiara R (2011b) Sarc3d: a new 3d body model for people tracking and re-identification. International Conference on Image Analysis and Processing pp 197–206

Bansal A, Nanduri A, Castillo C, Ranjan R, Chellappa R (2016) Umdfaces: An annotated face dataset for training deep networks. arXiv preprint arXiv:161101484

Bansal A, Castillo C, Ranjan R, Chellappa R (2017) The do's and don'ts for cnn-based face verification. In: Workshop of IEEE International Conference on Computer Vision

Belhumeur PN, Hespanha JP, Kriegman DJ (1997) Eigenfaces vs. fisherfaces: Recognition using class specific linear projection. IEEE Transactions on Pattern Analysis and Machine Intelligence 19(7):711–720

Bendale A, Boult T (2015) Towards open world recognition. In: IEEE Conference on Computer Vision and Pattern Recognition, pp 1893–1902

Bendale A, Boult TE (2016) Towards open set deep networks. In: IEEE Conference on Computer Vision and Pattern Recognition, pp 1563–1572

Berg T, Belhumeur PN (2013) Poof: Part-based one-vs.-one features for fine-grained categorization, face verification, and attribute estimation. In: IEEE Conference on Computer Vision and Pattern Recognition, pp 955–962

Best-Rowden L, Han H, Otto C, Klare BF, Jain AK (2014) Unconstrained face recognition: Identifying a person of interest from a media collection 9(12):2144–2157

Beveridge JR, Phillips PJ, Bolme DS, Draper BA, Givens GH, Lui YM, Teli MN, Zhang H, Scruggs WT, Bowyer KW, et al (2013) The challenge of face recognition from digital point-and-shoot cameras. In: IEEE International Conference on Biometrics: Theory, Applications, and Systems

Bilgazyev E, Efraty BA, Shah SK, Kakadiaris IA (2011) Sparse representation-based super resolution for face recognition at a distance. In: British Machine Vision Conference

Biswas S, Bowyer KW, Flynn PJ (2010) Multidimensional scaling for matching low-resolution facial images. In: IEEE International Conference on Biometrics: Theory, Applications, and Systems, pp 1–6

Biswas S, Bowyer KW, Flynn PJ (2012) Multidimensional scaling for matching low-resolution face images. IEEE Transactions on Pattern Analysis and Machine Intelligence 34(10):2019–2030

Bottou L (2010) Large-scale machine learning with stochastic gradient descent. In: COMPSTAT

Bruhn A, Weickert J, Schnörr C (2005) Lucas/kanade meets horn/schunck: Combining local and global optic flow methods. International Journal of Computer Vision 61(3):211–231

Cao Q, Lin L, Shi Y, Liang X, Li G (2017a) Attention-aware face hallucination via deep reinforcement learning. In: IEEE Conference on Computer Vision and Pattern Recognition

Cao Q, Shen L, Xie W, Parkhi OM, Zisserman A (2017b) Vggface2: A dataset for recognising faces across pose and age. arXiv preprint arXiv:171008092

Cao X, Wipf D, Wen F, Duan G, Sun J (2013) A practical transfer learning algorithm for face verification. In: IEEE International Conference on Computer Vision

Cao X, Wei Y, Wen F, Sun J (2014) Face alignment by explicit shape regression. International Journal of Computer Vision 107(2):177–190

Chakrabarti A, Rajagopalan A, Chellappa R (2007) Super-resolution of face images using kernel pca-based prior. IEEE Transactions on Multimedia 9(4):888–892

Chang KI, Bowyer KW, Flynn PJ (2005) An evaluation of multimodal 2d+ 3d face biometrics. IEEE Transactions on Pattern Analysis and Machine Intelligence 27(4):619–624

Chellappa R, Wilson CL, Sirohey S (1995) Human and machine recognition of faces: A survey. Proceedings of the IEEE 83(5):705–741

Chen D, Cao X, Wang L, Wen F, Sun J (2012) Bayesian face revisited: A joint formulation. European Conference on Computer Vision

Chen D, Cao X, Wen F, Sun J (2013) Blessing of dimensionality: High-dimensional feature and its efficient compression for face verification. In: IEEE Conference on Computer Vision and Pattern Recognition

Cheng DS, Cristani M, Stoppa M, Bazzani L, Murino V (2011) Custom pictorial structures for re-identification. In: British Machine Vision Conference

Choi JY, Ro YM, Plataniotis KN (2008) Feature subspace determination in video-based mismatched face recognition. In: IEEE Conference on Automatic Face and Gesture Recognition

Choi JY, Ro YM, Plataniotis KN (2009) Color face recognition for degraded face images 39(5):1217–1230

Das A, Chakraborty A, Roy-Chowdhury AK (2014) Consistent re-identification in a camera network. In: European Conference on Computer Vision

Daugman J (1997) Face and gesture recognition: Overview. IEEE Transactions on Pattern Analysis and Machine Intelligence 19(7):675–676

Dong C, Loy CC, He K, Tang X (2014) Learning a deep convolutional network for image super-resolution. In: European Conference on Computer Vision

Dong C, Loy CC, Tang X (2016) Accelerating the super-resolution convolutional neural network. In: European Conference on Computer Vision

Dong Q, Gong S, Zhu X (2017) Class rectification hard mining for imbalanced deep learning. In: IEEE Inter-

national Conference on Computer Vision, pp 1851–1860

Dong Q, Gong S, Zhu X (2018) Imbalanced deep learning by minority class incremental rectification. IEEE Transactions on Pattern Analysis and Machine Intelligence

Electron E (2017) Easenelectron. http://english.easen-electron.com/

Ersotelos N, Dong F (2008) Building highly realistic facial modeling and animation: a survey. Image and Vision Computing 24(1):13–30

Farhadi A, Endres I, Hoiem D, Forsyth D (2009) Describing objects by their attributes. In: IEEE Conference on Computer Vision and Pattern Recognition, pp 1778–1785

Fookes C, Lin F, Chandran V, Sridharan S (2012) Evaluation of image resolution and super-resolution on face recognition performance. Journal of Visual Communication and Image Representation 23(1):75–93

Frome A, Corrado GS, Shlens J, Bengio S, Dean J, Mikolov T, et al (2013) Devise: A deep visual-semantic embedding model. In: Advances in Neural Information Processing Systems, pp 2121–2129

Fu Y, Hospedales TM, Xiang T, Gong S (2014) Learning multimodal latent attributes. IEEE transactions on pattern analysis and machine intelligence 36(2):303–316

Fu Y, Xiang T, Jiang YG, Xue X, Sigal L, Gong S (2017) Recent advances in zero-shot recognition. IEEE Signal Processing Magazine

Gallagher AC, Chen T (2009) Understanding images of groups of people. In: IEEE Conference on Computer Vision and Pattern Recognition, pp 256–263

Ganin Y, Lempitsky V (2015) Unsupervised domain adaptation by backpropagation. In: International Conference on Machine learning, pp 1180–1189

Gao W, Cao B, Shan S, Chen X, Zhou D, Zhang X, Zhao D (2008) The cas-peal large-scale chinese face database and baseline evaluations 38(1):149–161

Gatys LA, Ecker AS, Bethge M (2016) Image style transfer using convolutional neural networks. In: IEEE Conference on Computer Vision and Pattern Recognition, pp 2414–2423

Georghiades AS, Belhumeur PN, Kriegman DJ (2001) From few to many: Illumination cone models for face recognition under variable lighting and pose. IEEE Transactions on Pattern Analysis and Machine Intelligence 23(6):643–660

Ghifary M, Kleijn WB, Zhang M, Balduzzi D, Li W (2016) Deep reconstruction-classification networks for unsupervised domain adaptation. In: European Conference on Computer Vision, pp 597–613

Gong S, MeKenna S, Psarrou A (2000) Dynamic Vision: From Images to Face Recognition. Imperial College Press, World Scientific

Gong S, Cristani M, Yan S, Loy CC (2014) Person re-identification. Springer

Gou M, Karanam S, Liu W, Camps O, Radke RJ (2017) Dukemtmc4reid: A large-scale multi-camera person re-identification dataset. In: Workshop of IEEE Conference on Computer Vision and Pattern Recognition

Gray D, Tao H (2008) Viewpoint invariant pedestrian recognition with an ensemble of localized features. European Conference on Computer Vision

Grgic M, Delac K, Grgic S (2011) Scface–surveillance cameras face database. Multimedia Tools and Applications 51(3):863–879

Gross R, Matthews I, Cohn J, Kanade T, Baker S (2010) Multi-pie. Image and Vision Computing 28(5):807–813

Grother P, Ngan M (2014) Face recognition vendor test (frvt): Performance of face identification algorithms. NIST Interagency Report 8009(5)

Grother P, Ngan M, Hanaoka K (2017) Face recognition vendor test (frvt) ongoing

Günther M, Hu P, Herrmann C, Chan CH, Jiang M, Yang S, Dhamija AR, Ramanan D, Beyerer J, Kittler J, et al (2017) Unconstrained face detection and open-set face recognition challenge. In: International Joint Conference on Biometrics

Gunturk BK, Batur AU, Altunbasak Y, Hayes MH, Mersereau RM (2003) Eigenface-domain super-resolution for face recognition. IEEE Transactions on Image Processing 12(5):597–606

Guo Y, Zhang L, Hu Y, He X, Gao J (2016a) Ms-celeb-1m: A dataset and benchmark for large-scale face recognition. In: European Conference on Computer Vision

Guo Y, Zhang L, Hu Y, He X, Gao J (2016b) MS-Celeb-1M: A dataset and benchmark for large scale face recognition. In: European Conference on Computer Vision, Springer

Hadsell R, Chopra S, LeCun Y (2006) Dimensionality reduction by learning an invariant mapping. In: IEEE Conference on Computer Vision and Pattern Recognition

He K, Zhang X, Ren S, Sun J (2016) Deep residual learning for image recognition. In: IEEE Conference on Computer Vision and Pattern Recognition

He X, Cai D, Yan S, Zhang HJ (2005) Neighborhood preserving embedding. In: IEEE International Conference on Computer Vision

Helbing D, Molnar P (1995) Social force model for pedestrian dynamics. Physical review E 51(5):4282

Hennings-Yeomans PH, Baker S, Kumar BV (2008) Simultaneous super-resolution and feature extraction for recognition of low-resolution faces. In: IEEE Conference on Computer Vision and Pattern Recognition

Hu P, Ramanan D (2016) Finding tiny faces. arXiv e-print

Huang C, Li Y, Change Loy C, Tang X (2016) Learning deep representation for imbalanced classification. In: IEEE Conference on Computer Vision and Pattern Recognition, pp 5375–5384

Huang GB, Learned-Miller E (2017) Labeled faces in the wild. http://vis-www.cs.umass.edu/lfw/results.html

Huang GB, Ramesh M, Berg T, Learned-Miller E (2007) Labeled faces in the wild: A database for studying face recognition in unconstrained environments. Tech. rep., University of Massachusetts

Huang Z, Shan S, Wang R, Zhang H, Lao S, Kuerban A, Chen X (2015) A benchmark and comparative study of video-based face recognition on cox face database. IEEE Transactions on Image Processing 24(12):5967–5981

Hughes RL (2002) A continuum theory for the flow of pedestrians. Transportation Research Part B: Methodological 36(6):507–535

Jia K, Gong S (2005) Multi-modal tensor face for simultaneous super-resolution and recognition. In: IEEE International Conference on Computer Vision

Jia K, Gong S (2008) Generalized face super-resolution. IEEE Transactions on Image Processing 17(6):873–886

Jiang J, Hu R, Wang Z, Han Z, Ma J (2016) Facial image hallucination through coupled-layer neighbor embedding. IEEE Transactions on Circuits and Systems for Video Technology 26(9):1674–1684

Jin Y, Bouganis CS (2015) Robust multi-image based blind face hallucination. In: IEEE Conference on Computer Vision and Pattern Recognition

K-S I, Seitz SM, Miller D, Brossard E (2016) The megaface benchmark: 1 million faces for recognition at scale. In: IEEE Conference on Computer Vision and Pattern Recognition

Kawanishi Y, Wu Y, Mukunoki M, Minoh M (2014) Shinpuhkan2014: A multi-camera pedestrian dataset for tracking people across multiple cameras. In: Korea-Japan Joint Workshop on Frontiers of Computer Vision

Kim J, Kwon Lee J, Mu Lee K (2016a) Accurate image super-resolution using very deep convolutional networks. In: IEEE Conference on Computer Vision and Pattern Recognition

Kim J, Kwon Lee J, Mu Lee K (2016b) Deeply-recursive convolutional network for image super-resolution. In: IEEE Conference on Computer Vision and Pattern Recognition

Kim KI, Kwon Y (2010) Single-image super-resolution using sparse regression and natural image prior. IEEE Transactions on Pattern Analysis and Machine Intelligence 32(6):1127–1133

Klare BF, Klein B, Taborsky E, Blanton A, Cheney J, Allen K, Grother P, Mah A, Jain AK (2015) Pushing the frontiers of unconstrained face detection and recognition: Iarpa janus benchmark a. In: IEEE Conference on Computer Vision and Pattern Recognition

Kong SG, Heo J, Abidi BR, Paik J, Abidi MA (2005) Recent advances in visual and infrared face recognitiona review. Computer Vision and Image Understanding 97(1):103–135

Krizhevsky A, Sutskever I, Hinton GE (2012) Imagenet classification with deep convolutional neural networks. In: Advances in Neural Information Processing Systems

Kumar N, Berg AC, Belhumeur PN, Nayar SK (2009) Attribute and simile classifiers for face verification. In: IEEE International Conference on Computer Vision, pp 365–372

Lai WS, Huang JB, Ahuja N, Yang MH (2017) Deep laplacian pyramid networks for fast and accurate super-resolution. In: IEEE Conference on Computer Vision and Pattern Recognition

Ledig C, Theis L, Huszár F, Caballero J, Cunningham A, Acosta A, Aitken A, Tejani A, Totz J, Wang Z, et al (2016) Photo-realistic single image super-resolution using a generative adversarial network. arXiv e-print

Lee CY, Xie S, Gallagher P, Zhang Z, Tu Z (2015) Deeply-supervised nets. In: Artificial Intelligence and Statistics, pp 562–570

Lei Z, Ahonen T, Pietikäinen M, Li SZ (2011) Local frequency descriptor for low-resolution face recognition. In: IEEE Conference on Automatic Face and Gesture Recognition

Li B, Chang H, Shan S, Chen X, Gao W (2008) Hallucinating facial images and features. In: IEEE International Conference on Pattern Recognition

Li B, Chang H, Shan S, Chen X (2009) Coupled metric learning for face recognition with degraded images. Advances in Machine Learning

Li B, Chang H, Shan S, Chen X (2010) Low-resolution face recognition via coupled locality preserving mappings 17(1):20–23

Li C, Wand M (2016) Precomputed real-time texture synthesis with markovian generative adversarial networks. In: European Conference on Computer Vision, pp 702–716

Li S, Jain A (2011) Handbook of Face Recognition. Springer

Li W, Zhao R, Xiao T, Wang X (2014) Deepreid: Deep filter pairing neural network for person re-identification. In: IEEE Conference on Computer Vision and Pattern Recognition

Li Y, Fang C, Yang J, Wang Z, Lu X, Yang MH (2017) Diversified texture synthesis with feed-forward networks. In: IEEE Conference on Computer Vision and Pattern Recognition

Liao S, Lei Z, Yi D, Li SZ (2014) A benchmark study of large-scale unconstrained face recognition. In: International Joint Conference on Biometrics

Liu C, Wechsler H (2002) Gabor feature based classification using the enhanced fisher linear discriminant model for face recognition. IEEE Transactions on Image Processing 11(4):467–476

Liu C, Shum HY, Freeman WT (2007) Face hallucination: Theory and practice. International Journal of Computer Vision 75(1):115

Liu J, Deng Y, Bai T, Wei Z, Huang C (2015a) Targeting ultimate accuracy: Face recognition via deep embedding. arXiv e-print

Liu K, Ma B, Zhang W, Huang R (2015b) A spatio-temporal appearance representation for viceo-based pedestrian re-identification. In: IEEE International Conference on Computer Vision

Liu TY, et al (2009) Learning to rank for information retrieval. Foundations and Trends® in Information Retrieval 3(3):225–331

Liu W, Lin D, Tang X (2005) Hallucinating faces: Tensorpatch super-resolution and coupled residue compensation. In: IEEE Conference on Computer Vision and Pattern Recognition

Liu W, Wen Y, Yu Z, Li M, Raj B, Song L (2017) Sphereface: Deep hypersphere embedding for face recognition. In: IEEE Conference on Computer Vision and Pattern Recognition

Liu Z, Luo P, Wang X, Tang X (2015c) Deep learning face attributes in the wild. In: IEEE International Conference on Computer Vision

Loy CC, Xiang T, Gong S (2009) Multi-camera activity correlation analysis. In: IEEE Conference on Computer Vision and Pattern Recognition

Lu C, Tang X (2015) Surpassing human-level face verification performance on lfw with gaussianface. In: AAAI Conference on Artificial Intelligence

Maltoni D, Maio D, Jain A, Prabhakar S (2009) Handbook of fingerprint recognition. Springer Science & Business Media

Manyam OK, Kumar N, Belhumeur P, Kriegman D (2011) Two faces are better than one: Face recognition in group photographs. In: International Joint Conference on Biometrics, pp 1–8

Martinel N, Micheloni C (2012) Re-identify people in wide area camera network. In: Workshop of IEEE Conference on Computer Vision and Pattern Recognition

Masi I, Rawls S, Medioni G, Natarajan P (2016) Pose-aware face recognition in the wild. In: IEEE Conference on Computer Vision and Pattern Recognition

Messer K, Matas J, Kittler J, Luettin J, Maitre G (1999) Xm2vtsdb: The extended m2vts database. In: International Conference on Audio and Video-based Biometric Person Authentication

Nech A, K-S I (2017) Level playing field for million scale face recognition. In: IEEE Conference on Computer Vision and Pattern Recognition

Ng HW, Winkler S (2014) A data-driven approach to cleaning large face datasets. In: IEEE International Conference on Image Processing

Ortiz EG, Becker BC (2014) Face recognition for web-scale datasets. Computer Vision and Image Understanding 118:153–170

Pan SJ, Yang Q (2010) A survey on transfer learning. IEEE Transactions on Knowledge and Data Engineering 22(10):1345–1359

Parikh D, Grauman K (2011) Relative attributes. In: IEEE International Conference on Computer Vision, pp 503–510

Parkhi OM, Vedaldi A, Zisserman A (2015) Deep face recognition. In: British Machine Vision Conference

Phillips PJ, Moon H, Rizvi SA, Rauss PJ (2000) The feret evaluation methodology for face-recognition algorithms. IEEE Transactions on Pattern Analysis and Machine Intelligence 22(10):1090–1104

Phillips PJ, Flynn PJ, Scruggs T, Bowyer KW, Chang J, Hoffman K, Marques J, Min J, Worek W (2005) Overview of the face recognition grand challenge. In: IEEE Conference on Computer Vision and Pattern Recognition

Phillips PJ, Scruggs WT, O'Toole AJ, Flynn PJ, Bowyer KW, Schott CL, Sharpe M (2010) Frvt 2006 and ice 2006 large-scale experimental results. IEEE Transactions on Pattern Analysis and Machine Intelligence 32(5):831–846

Prado KS, Roman NT, Silva VF, Bernardes Jr JL, Digiampietri LA, Ortega EM, Lima CA, Cura LM, Antunes MM (2016) Automatic facial recognition: A systematic review on the problem of light variation

Ren CX, Dai DQ, Yan H (2012) Coupled kernel embedding for low-resolution face image recognition. IEEE Transactions on Image Processing 21(8):3770–3783

Ricanek K, Tesafaye T (2006) Morph: A longitudinal image database of normal adult age-progression. In: IEEE Conference on Automatic Face and Gesture

Recognition

Roth PM, Hirzer M, Köstinger M, Beleznai C, Bischof H (2014) Mahalanobis Distance Learning for Person Re-Identification. In: Person Re-Identification, Springer, pp 247–267

Rumelhart DE, Hinton GE, Williams RJ, et al (1988) Learning representations by back-propagating errors. Cognitive Modeling 5(3):1

Saenko K, Kulis B, Fritz M, Darrell T (2010) Adapting visual category models to new domains. European Conference on Computer Vision pp 213–226

Samal A, Iyengar PA (1992) Automatic recognition and analysis of human faces and facial expressions: A survey. Pattern Recognition 25(1):65–77

Samaria FS, Harter AC (1994) Parameterisation of a stochastic model for human face identification. In: IEEE Workshop on Applications of Computer Vision

Sarkar S, Phillips PJ, Liu Z, Vega IR, Grother P, Bowyer KW (2005) The humanid gait challenge problem: Data sets, performance, and analysis. IEEE Transactions on Pattern Analysis and Machine Intelligence 27(2):162–177

Schroff F, Kalenichenko D, Philbin J (2015) Facenet: A unified embedding for face recognition and clustering. In: IEEE Conference on Computer Vision and Pattern Recognition

Schwartz W, Davis L (2009) Learning discriminative appearance-based models using partial least squares. In: Brazilian Symposium on Computer Graphics and Image Processing

Sengupta S, Chen JC, Castillo C, Patel VM, Chellappa R, Jacobs DW (2016) Frontal to profile face verification in the wild. In: IEEE Winter Conference on Applications of Computer Vision

Shekhar S, Patel VM, Chellappa R (2011) Synthesis-based recognition of low resolution faces. In: International Joint Conference on Biometrics

Sim T, Baker S, Bsat M (2002) The cmu pose, illumination, and expression (pie) database. In: IEEE Conference on Automatic Face and Gesture Recognition, pp 53–58

Simonyan K, Zisserman A (2015) Very deep convolutional networks for large-scale image recognition. In: International Conference on Learning Representations

Song F, Tan X, Chen S (2014) Exploiting relationship between attributes for improved face verification. Computer Vision and Image Understanding 122:143–154

Song G, Leng B, Liu Y, Hetang C, Cai S (2017) Region-based quality estimation network for large-scale person re-identification. arXiv preprint arXiv:171108766

Sun Y, Chen Y, Wang X, Tang X (2014a) Deep learning face representation by joint identification-verification. In: Advances in Neural Information Processing Systems

Sun Y, Wang X, Tang X (2014b) Deep learning face representation from predicting 10,000 classes. In: Proceedings of the IEEE Conference on Computer Vision and Pattern Recognition, pp 1891–1898

Sun Y, Wang X, Tang X (2014c) Deep learning face representation from predicting 10,000 classes. In: IEEE Conference on Computer Vision and Pattern Recognition

Sun Y, Liang D, Wang X, Tang X (2015a) Deepid3: Face recognition with very deep neural networks. arXiv e-print

Sun Y, Wang X, Tang X (2015b) Deeply learned face representations are sparse, selective, and robust. In: IEEE Conference on Computer Vision and Pattern Recognition

Szegedy C, Liu W, Jia Y, Sermanet P, Reed S, Anguelov D, Erhan D, Vanhoucke V, Rabinovich A (2015) Going deeper with convolutions. In: IEEE Conference on Computer Vision and Pattern Recognition

Szegedy C, Ioffe S, Vanhoucke V, Alemi AA (2017) Inception-v4, inception-resnet and the impact of residual connections on learning. In: AAAI Conference on Artificial Intelligence

Tai Y, Yang J, Liu X (2017) Image super-resolution via deep recursive residual network. In: IEEE Conference on Computer Vision and Pattern Recognition

Taigman Y, Yang M, Ranzato M, Wolf L (2014) Deepface: Closing the gap to human-level performance in face verification. In: IEEE Conference on Computer Vision and Pattern Recognition

Taigman Y, Yang M, Ranzato M, Wolf L (2015) Webscale training for face identification. In: IEEE Conference on Computer Vision and Pattern Recognition

Tan X, Triggs B (2010) Enhanced local texture feature sets for face recognition under difficult lighting conditions. IEEE Transactions on Image Processing 19(6):1635–1650

Tan X, Chen S, Zhou ZH, Zhang F (2006) Face recognition from a single image per person: A survey. Pattern Recognition 39(9):1725–1745

Tencent (2017) Youtu lab, tencent. http://bestimage.qq.com/

Turk M, Pentland A (1991) Eigenfaces for recognition. Journal of Cognitive Neuroscience 3(1):71–86

Tzeng E, Hoffman J, Darrell T, Saenko K (2015) Simultaneous deep transfer across domains and tasks. In: IEEE International Conference on Computer Vision, pp 4068–4076

Wang D, Otto C, Jain AK (2016a) Face search at scale. IEEE Transactions on Pattern Analysis and Machine Intelligence

Wang T, Gong S, Zhu X, Wang S (2014a) Person re-identification by video ranking. In: European Conference on Computer Vision

Wang X, Tang X (2003) Face hallucination and recognition. In: International Conference on Audio-and Video-Based Biometric Person Authentication

Wang X, Tang X (2005) Hallucinating face by eigentransformation 35(3):425–434

Wang Z, Miao Z (2008) Scale invariant face recognition using probabilistic similarity measure. In: IEEE International Conference on Pattern Recognition

Wang Z, Miao Z, Wu QJ, Wan Y, Tang Z (2014b) Low-resolution face recognition: a review. Image and Vision Computing 30(4):359–386

Wang Z, Chang S, Yang Y, Liu D, Huang TS (2016b) Studying very low resolution recognition using deep networks. In: IEEE Conference on Computer Vision and Pattern Recognition

Wechsler H (2009) Reliable face recognition methods: system design, implementation and evaluation, vol 7. Springer Science & Business Media

Wechsler H, Philips J, Bruce V, Fogelman-Soulie F, Huang T (1998) Face Recognition: From Theory to Applications. Springer-Verlag

Wechsler H, Phillips JP, Bruce V, Soulie FF, Huang TS (2012) Face recognition: From theory to applications, vol 163. Springer Science & Business Media

Wen Y, Zhang K, Li Z, Qiao Y (2016) A discriminative feature learning approach for deep face recognition. In: European Conference on Computer Vision

Whitelam C, Taborsky E, Blanton A, Maze B, Adams J, Miller T, Kalka N, Jain AK, Duncan JA, Allen K, et al (2017) Iarpa janus benchmark-b face dataset. In: CVPR Workshop on Biometrics

Wolf L, Levy N (2013) The svm-minus similarity score for video face recognition. In: IEEE Conference on Computer Vision and Pattern Recognition

Wolf L, Hassner T, Maoz I (2011) Face recognition in unconstrained videos with matched background similarity. In: IEEE Conference on Computer Vision and Pattern Recognition

Wong Y, Sanderson C, Mau S, Lovell BC (2010) Dynamic amelioration of resolution mismatches for local feature based identity inference. In: IEEE International Conference on Pattern Recognition

Wright J, Yang AY, Ganesh A, Sastry SS, Ma Y (2009) Robust face recognition via sparse representation. IEEE Transactions on Pattern Analysis and Machine Intelligence 31(2):210–227

Xiao T, Li S, Wang B, Lin L, Wang X (2016) End-to-end deep learning for person search. arXiv e-print

Xie S, Tu Z (2015) Holistically-nested edge detection. In: IEEE International Conference on Computer Vision, pp 1395–1403

Xu X, Liu W, Li L (2013) Face hallucination: How much it can improve face recognition. In: Australian Conference

Yang CY, Ma C, Yang MH (2014) Single-image super-resolution: A benchmark. In: European Conference on Computer Vision

Yang J, Wright J, Huang TS, Ma Y (2010) Image super-resolution via sparse representation. IEEE Transactions on Image Processing 19(11):2861–2873

Yi D, Lei Z, Liao S, Li SZ (2014) Learning face representation from scratch. arXiv e-print

Yu X, Porikli F (2016) Ultra-resolving face images by discriminative generative networks. In: European Conference on Computer Vision

Yu X, Porikli F (2017) Hallucinating very low-resolution unaligned and noisy face images by transformative discriminative autoencoders. In: IEEE Conference on Computer Vision and Pattern Recognition

Zeiler MD, Fergus R (2014) Visualizing and understanding convolutional networks. In: European Conference on Computer Vision

Zhang B, Shan S, Chen X, Gao W (2007) Histogram of gabor phase patterns (hgpp): A novel object representation approach for face recognition. IEEE Transactions on Image Processing 16(1):57–68

Zhang K, Zhang Z, Li Z, Qiao Y (2016) Joint face detection and alignment using multitask cascaded convolutional networks. IEEE Signal Processing Letters 23(10):1499–1503

Zhang Z, Luo P, Loy CC, Tang X (2014) Facial landmark detection by deep multi-task learning. In: European Conference on Computer Vision, pp 94–108

Zhao W, Chellappa R (2011) Face Processing: Advanced modeling and methods. Academic Press

Zhao W, Chellappa R, Phillips PJ, Rosenfeld A (2003) Face recognition: A literature survey. ACM Computing Surveys 35(4):399–458

Zheng L, Shen L, Tian L, Wang S, Wang J, Tian Q (2015) Scalable person re-identification: A benchmark. In: IEEE International Conference on Computer Vision

Zheng WS, Gong S, Xiang T (2009) Associating groups of people. In: British Machine Vision Conference, vol 2

Zheng WS, Gong S, Xiang T (2016) Towards open-world person re-identification by one-shot group-based verification. IEEE Transactions on Pattern

Analysis and Machine Intelligence 38(3):591–606

Zhou C, Zhang Z, Yi D, Lei Z, Li SZ (2011) Low-resolution face recognition via simultaneous discriminant analysis. In: International Joint Conference on Biometrics

Zhou SK, Chellappa R, Zhao W (2006) Unconstrained face recognition, vol 5. Springer Science & Business Media

Zhu JY, Park T, Isola P, Efros AA (2017) Unpaired image-to-image translation using cycle-consistent adversarial networks. In: IEEE International Conference on Computer Vision

Zhu S, Li C, Change Loy C, Tang X (2015) Face alignment by coarse-to-fine shape searching. In: IEEE Conference on Computer Vision and Pattern Recognition, pp 4998–5006

Zhu S, Liu S, Loy CC, Tang X (2016) Deep cascaded bi-network for face hallucination. In: European Conference on Computer Vision

Zou WW, Yuen PC (2012) Very low resolution face recognition problem. IEEE Transactions on Image Processing 21(1):327–340

Zou X, Kittler J, Messer K (2007) Illumination invariant face recognition: A survey. In: IEEE International Conference on Biometrics: Theory, Applications, and Systems, pp 1–8